Multi-Aerial Robotic System for Power Line Inspection and Maintenance: Comparative Analysis from the AERIAL-CORE Final Experiments

A. Ollero, Fellow, IEEE, A. Suarez, C. Papaioannidis, I. Pitas, Life Fellow, IEEE, J.M. Marredo, V. Duong, student member, IEEE, E. Ebeid, Senior member, IEEE, V. Krátký, M. Saska, C. Hanoune, A. Afifi, A. Franchi, Fellow, IEEE, C. Vourtsis, D. Floreano, Fellow, IEEE, G. Vasiljevic, member, IEEE, S. Bogdan, Senior member, IEEE, A. Caballero, F. Ruggiero, Senior member, IEEE, V. Lippiello, Senior member, IEEE, C. Matilla, G. Cioffi, Student member, IEEE, D. Scaramuzza, Senior member, IEEE, J. R. Martinez-de Dios, B. C. Arrue, Senior member, IEEE, C. Martín, K. Zurad, C. Gaitán, J. Rodriguez, A. Munoz, A. Viguria, Senior member, IEEE *

Abstract

This paper shows how different types of novel aerial robots with new functionalities can cooperate in the inspection and maintenance (I&M) of power lines, one of the largest and most essential civil infrastructures in any country. This study relies on the results from the AERIAL-CORE research and innovation project. The paper describes an I&M validation scenario and evaluation metrics for three linked operation domains: 1) long-range inspection for the detection of possible damages on power lines in a post-storm scenario, 2) aerial manipulation for the installation of devices on power lines, and 3) aerial co-working to help human operators in their activities at height. It presents the demonstration of ten different aerial robots in a real scenario with 10 km of power lines. The platforms include morphing-wing and VTOL (vertical take-off and landing) UAVs (unmanned aerial vehicles), multi-rotors, and aerial manipulators. These platforms, custom-developed or commercially available, are evaluated in the three application domains, describing the new functionalities implemented for each case. The paper ends with guidelines, design principles, and lessons learned for future developments derived from the final demonstration of the project.

Multimedia

A video summarizing the AERIAL-CORE project can be found at `https://www.youtube.com/watch?v=0yw7VwM7sCs`.

1 Introduction

The power grid is nowadays one of the most critical civil infrastructures in any country, providing continuous service to hundreds of millions of users along tens of millions of km. It is

*This work was supported by the European Union's Horizon 2020 Research and Innovation Program under grant agreement no. 871479 (AERIAL-CORE).

estimated that there are around 72 million km of high-voltage power lines worldwide according to the International Energy Agency (IEA)[1]. The continuous exposure of this infrastructure to adverse climatic conditions (wind, rain, snow, ice, temperature variations), as well as the interference with the surrounding vegetation and birdlife, among other factors, makes the realization of periodic inspection and maintenance (I&M) tasks essential to guarantee the continuous service and to ensure the fast recovery against blackouts caused for example by storms. Climate change is increasing the rate of natural disasters and more adverse weather conditions that usually damage electrical transmission towers and cables. Furthermore, I&M activities are necessary to prevent possible faults and environmental damages, requiring, for example, preventive pruning to avoid fires caused by tree branches close to power lines, as well as to protect bird species from collision or electrocution, which can also cause power cuts, power outages, and start fires during periods of drought.

The realization of I&M activities on power lines is particularly difficult, risky for humans, and costly (total inspection and maintenance cost in Europe has been estimated at more than 2.2 billion €/year) due to three main reasons: (1) the high altitude of the cables, from 10 up to 50 m, (2) the high voltage, in the range of tens or hundreds of kilovolts, and (3) the vast extension of the grid, making in some cases difficult to detect the source of a fault. Conventional inspection campaigns, involving two or three qualified operators, are very costly due to the need to use vehicles like vans with elevated work platforms, or manned helicopters with a cost of around 150 €/km. Maintenance activities are even more expensive and highly risky as these involve the direct operation of human workers on the power line, requiring in some cases the disconnection of some section of the line, with the consequent loss of service during operation.

The inspection and maintenance of the power grid requires the realization of a number of operations to ensure continuous service, comprising periodic inspection campaigns, specific maintenance actions, as well as repair jobs. Some examples of activities carried out by companies include: periodic visual inspection to measure the vegetation growth and conduct preventive pruning to avoid possible fires; visual inspection of elements like insulators, screws, and nuts to detect corrosion; identification of broken cables; or detection of fallen trees, bent towers due to wind, or plastic and fabric sheets tangled in the cables. Activities that require direct actuation from workers include: cleaning insulators, de-icing cables, and installation of devices on the lines such as electrical spacers, vibration dampers, anti-nest devices, or bird diverters, imposed by regulation to protect avian species from collision or electrocution.

Visual, infrared, or LiDAR-based inspection are done by taking high-resolution pictures or point clouds of specific power line sections or towers, accessed typically by walking or using ground vehicles, helicopters, or manned ground vehicles. These data are later post-processed to generate the reports that determine the maintenance actions based on the identified defects. The human intervention involved in the data acquisition, annotation and processing makes the inspection process slow, particularly given the extension of the power grid, which motivates the application of aerial robots with cognitive capabilities, as proposed in the AERIAL-CORE project, which has been considered a "success case" by the European Commission. Conversely, the realization of maintenance operations, like the installation of devices as those considered in [1], requires physical contact with the power lines. Human workers may reach the workspace by climbing the towers, through elevated working platforms (see Figure 1), or with manned helicopters. However, the risk of an injury is significant, especially when operating with live power lines at tens or hundreds of kilovolts.

The difficulty in accessing the power lines due to their altitude motivates the use of aerial robots equipped with robotic arms and end effectors [2] to perform maintenance tasks [1]. Aerial robots may also help human workers deployed on-site as depicted in Figure 1, e.g., by transmitting images of the workers' activity to ensure safety, or serving as delivery platforms

[1] `https://www.iea.org/reports/sustainable-recovery/electricity`

to provide tools or devices from a supply point.

Figure 1: Human operator on elevated working platform grounding the three phases of a power line section close to the ATLAS Flight Center before conducting a maintenance task.

The AERIAL-CORE project explored the research, development, and application of novel methods and technologies designed to automate the realization of inspection and maintenance (I&M) operations on power grids consisting of several power-lines, using aerial robots for this purpose. The project life cycle comprised several phases and activities. The desired requirements and specifications for the power-lines I&M solution were provided in the first place by the end user, which is in this case one of the main electric companies managing the power grid in Europe, followed by the analysis of existing procedures, technologies, and other research works. The specifications have been also discussed with the members of the Industrial Advisory Committee of the project, including other relevant companies. The platforms and methods were designed and developed based on the definition of use cases, distinguishing three subsystems in AERIAL-CORE: long-range inspection, local aerial manipulation, and aerial co-worker. This follows a logical and practical approach to the realization of I&M activities. Those methods and prototypes that achieved a higher TRL (technology readiness level) were selected for validation in a real power line scenario, under the supervision of the electric company. The dissemination of the results obtained in the project, presented here, is essential to promote the exploitation of aerial robots and their benefits for this application, contributing to its widespreadity in different scenarios.

The main contribution of the paper is the performance evaluation and comparison of different types of novel aerial robotics and manipulation platforms (10 in total) incorporating perception, mapping, planning, and manipulation methods, developed for the inspection and maintenance of power lines based on the results and knowledge derived from the AERIAL-CORE project final demonstration (October 2023). The platforms involved in these experiments are shown in Figure 2, indicating, for comparative purposes, some of their specifications in Table 1. The paper proposes a unified approach to present the features and capabilities of these platforms and evaluate their performance qualitatively and quantitatively.

The rest of the paper is organized as follows. Section 2 introduces other robotic technologies for power line I&M based on literature surveys. Section 3 describes the scenarios and evaluation procedures proposed in this paper. Section 4 presents the developed platforms for the three operation domains (long-range, manipulation, and aerial co-worker), describing on Sections 5, 6, and 7 the functionalities and results on these three domains. The paper concludes with lessons learned and recommendations in Section 8, and a summary of the results in Section 9.

Figure 2: Aerial robotic platforms in the AERIAL-CORE final demonstrations, organized according to the operation domains.

Table 1: Main features of the robotic platforms involved in the AERIAL-CORE project final demonstration. Nominal flight speed in [m/s], max. flight time in [min], max. flight range in [km], weight in [kg], power consumption in [W]. Acronyms: Functionalities (FU), Capabilities (CA), 3D LiDAR (L), Visual Camera (VC), High Resolution Visual Camera (HRVC), Infrared camera (IRC), LiDAR semantic Mapping (LSM), Visual Inspection (VINS), Morphing (MO), Wing Morphing (WMO), Device Installation (DIN), Perching and Rolling (PR), Dual Arm Manipulation (DAM), Detail Inspector (D-Ins), Safety-Co-Worker (Safe-CW)

Domain	Platform	Type	FC and CA	Speed	Time	Range	Weight	Power	Sensors
Long Range Inspection	Marvin	Product	VTOL, WMO, VINS	15	60	70	6.4	2000	L, HRVC, IRC
	Morpho	Prototype	VTOL, WMO, VINS	18.8	3.2	0.82	3.5	2000	VC
	DeltaQuad	Product	VTOL, VINS	18	120	120	6.2	2000	VC
	Mapper	Custom	LSM	10	15	5	15.6	2000	L, VC, GPS
	D-Ins	Product	VINS, recharging	10	30	10	4.8	800	HRVC, IRC, GPS
Aerial Manipulation	DARP	Prototype	DAM, PR, DIN	2	10	0.5	8	1000	RTK GPS
	MLMP	Prototype	DIN, PR	1.5	17	0.5	45	6400	2 L, IMU
Aerial CoWorker	ACW-V	Prototype	Line voltage check	1	10	0.3	4	1000	L
	ACW-D	Prototype	Delivery to humans	1	5	0.15	5	850	L, RGB-D
	Safe-CW	Prototype	Safe Co-working	10	18	6	3.5	1200	L, RTK GPS, VC

2 Literature Review and Existing Solutions

Surveys on power line inspection robots [3, 4] classify robots in three main categories depending on the locomotion method: climbing, aerial, and hybrid climbing-aerial. Climbing robots are rolling platforms that are deployed on the power line typically to perform some kind of detailed inspection operation of the cable or the installation of devices. One of the main challenges addressed with this kind of platforms is how to overcome obstacles on the line, including installed devices and the towers. Several climbing robots with limbs capable of grab-release the cables and overcome obstacles have been proposed (see [3] for a detailed comparison), although most effort has been devoted to the locomotion problem, resulting in complex, slow, and heavy mechanisms. The deployment of this type of robots also becomes more difficult and physically demanding for human workers as the weight is higher. The comparison between climbing and flying robots presented in [3] and [5] points out the mechanical complexity of climbing robots compared to UAVs for inspection operations.

Before the rise of multi-rotor aerial platforms in the 2010 decade, the use of automated helicopters for inspection of power lines was investigated in several works [5], reporting some inconveniences related to image blurring due to the vibrations of fuel engines and the low frame rate of the on-board image processing due to technological limitations back then. A complete

literature review on perception for power transmission lines inspection robots is presented in [6], evidencing the diverse challenges, technologies, and methods for 3D reconstruction, object detection, and visual servoing. Work [4] organizes the perception methods according to the inspected component, carrying platform (climbing or aerial), type of sensor, and applied method (image processing, deep learning, and others).

Some commercial robots for power line inspection can be found, remarking the LineScout and the LineRanger climbing robot[2] (45 kg weight) from Hydro - Québec that is deployed on the power line through cables handled by human workers. Other commercial robots for maintenance operations are the CSR-18 Robot (40 kg weight) developed by PLP and FulcrumAir for the installation of electrical spacers[3] (150 devices per day), tested on 240 kV lines, requiring deployment from elevated working platforms, and the Mini LineFly Robot[4] (10 kg) from the same companies, devoted to the installation of helical bird diverters (up to 400 devices per day), deployed on the line by means of a coaxial aerial platform. However, these aerial robots are teleoperated, which imposes significant operational constraints.

Although fully autonomous aerial robots have been successfully validated in relevant industrial applications and environments [7, 8, 9], their use for power line I&M introduces some specific requirements, which are not jointly met by any aerial robotic system:

- The huge extension and high degree of branching of the power grid make necessary the implementation of appropriate planning methods for single or multi-UAV systems to execute missions minimizing the operation time taking into account the wind effect and several other requirements and constraints (see [10] and its references).
- The autonomous visual detection and tracking of power lines using UAVs is not trivial due to the small thickness of the cables and the need to estimate the relative distance while flying [11, 12].
- The automatic detection of elements of interest in a power line scenario from LiDAR data requires specific methods to segment semantically and classify the towers, cables, and surrounding vegetation [13, 14].
- Aerial robots physically interacting with live power lines at tens or hundreds of kilovolts have to deal with electrostatic discharge and other electromagnetic compatibility problems [15, 16].
- Aerial robots can recharge their batteries to extend the degree of autonomy and operation time by incorporating energy harvesting mechanisms [17, 18].
- Aerial robots should be able to collaborate with human workers, involving physical interaction [19] for delivery of tools or devices [20], as well as visual gesture recognition [21, 22] to monitor safety conditions of human operators deployed on the power lines.

Therefore, the autonomous aerial robotic system to be used in I&M of power lines requires advanced functionalities (perception, localization, navigation, planning) to provide higher decisional autonomy in the realization of the tasks. The implementation of these functionalities contributes to reducing significantly the operation time while increasing the area coverage and number of locations that can be accessed. Given the extension of the power line scenarios, it is interesting to explore the deployment of different platforms combining manoeuvrability with endurance and the ability of recharging the batteries autonomously from the power line by induction, as well as hybrid solutions combining aerial platform with rolling base to increase the energy efficiency [23].

[2]LineRanger robot: `https://www.youtube.com/watch?v=OItActG9S6U`
[3]CSR-TWIN Robot: `https://www.youtube.com/watch?v=WGL74Xm5_cw`
[4]Mini LineFly Robot: `https://www.youtube.com/watch?v=wIzXruC6Xto`

3 Methodology for the Evaluation of Power Line I&M Aerial Robotic Systems

In this section, we introduce a methodology for evaluating the performance of aerial robotic systems in power line I&M operations. Although the technologies and methods described in this paper represent particular implementations in the context of the AERIAL-CORE project, the approach, taking inspiration from our previous works in benchmarking for aerial robotics [24] and [25], can be applied to evaluate other I&M aerial robotic solutions. Given the diversity of research and commercial robots that have been developed [3, 4] or can be employed in power line I&M, it is convenient to define a methodology to evaluate the performance of the aerial robotic systems. This methodology comprises the definition of the scenario, the operation domains, the requirements and parameters, and the metrics for each operation domain.

The considered evaluation scenario is a post-storm situation in which a certain area of the power grid is suspected to be affected by failures, such as the presence of some plastic fabric tangled in the cables, missing devices on the power line, or vegetation in close proximity to the power line due to the effect of wind. Other scenarios, such as regular inspections for preventive maintenance, can be considered but are not included in the paper. The general methodology for the I&M of power lines comprises:

- Inspection of a given geographical area covering a number of power lines and towers by using aerial robots;
- Maintenance in which two different approaches can be adopted: i) using aerial robots not cooperating with humans and ii) robots co-working with humans, assisting human operators in complex maintenance activities (by performing power line voltage check, tool delivery, monitoring, and on-demand inspection).

Figure 3 shows the three operation domains considered in the power lines I&M scenario: Long-Range Inspection, Local Aerial Manipulation, and Aerial Co-worker.

This classification obeys the logical approach followed when a failure on the power grid occurs: localize the failure or problem by deploying the aerial robots to inspect a certain area in the range of kilometres, then conduct the maintenance operations on a particular power line section using the aerial robots alone, or in collaboration with human operators. Two operation domains are considered: Local Aerial Manipulation for the installation of devices on the power lines; and Aerial Co-Working for assisting the human operators in maintenance activities when these activities are too complex to be performed reliably by the aerial robots. The next three subsections are focused on these operation domains

The involved platforms developed in AERIAL-CORE for each operation domain are summarized in Section 4. The functionalities and experimental results in each of three operation domains are briefly summarized in Sections 5, 6, and 7, respectively.

3.1 Long-Range Inspection

The aerial robotic system performs fully autonomously the visual detection and mapping along several kilometres of power lines using aerial robots. The long-range inspection is executed on a given area of the power grid, including several power line segments and electrical towers whose position and altitude can be determined from the GNSS (global navigation satellite system) coordinates obtained from maps and/or geolocalization services. Visual, thermal and/or LiDAR-based inspection of the power grid area is performed to detect possible faults or defects in the post-storm scenario, as well as excessive vegetation growth. The Long-Range Inspection operation domain, represented in Figure 3-Left, includes the Ground Control Station (GCS)

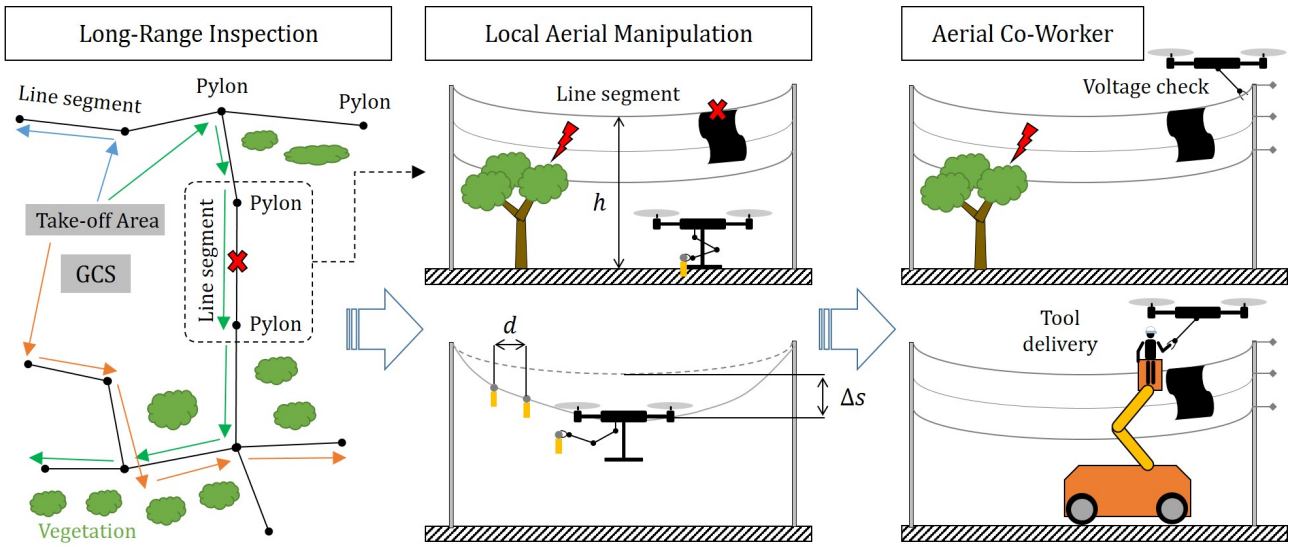

Figure 3: The three operation domains considered in the validation scenario: Long-Range Inspection (left), Local Aerial Manipulation (center), Aerial Co-Worker (right).

from which the aerial robotic system is managed; the take-off area from which the platforms are deployed and land; the line segments detected as affected by the fault; and the vegetation volumes that may represent a risk of fire due to excessive proximity to the power lines.

The requirements and parameters involved in the operation include the power grid area to be inspected, given by the coordinates of a corresponding pair of towers for each power line section; the location of the take-off and landing areas; the list of aerial platforms and their features (maximum speed, flight time and range, weight, power consumption) involved in the planning of the multi-UAV inspection operation; and a list of constraints regarding maximum/minimum flight altitude, safety distances from the power lines and towers for collision avoidance.

The metrics of interest for evaluating the performance of the long-range inspection platforms are the following: accuracy of the acquired images (Ground Sampling Distance, GSD, in mm/pixel); ability to perform the inspection fully autonomously including line tracking, without the intervention of any human operator; mean lifetime of the line tracker; semantic LiDAR-based map metrics (mean mapping error in cm and the Precision, Recall and F1 Score of the semantic mapping classification); number of km of power lines inspected (in a single fly); the time required to perform the inspection of the power grid (from take-off to landing, for each platform and/or for the complete UAV fleet) and the average time required to detect and localise the failure in the power grid. Additionally, the time required to compute the mission plan in the multi-UAV system is also considered.

As will be pointed out in the next sections, multi-rotors and hybrid fixed-wing/rotary-wing platforms can be applied to implement a cooperative inspection mission with a planning system that exploits the capabilities of the different platforms to increase the effectiveness of the fleet to localize failures in a short time.

3.2 Local Aerial Manipulation

This operation domain involves the installation of devices like bird flight diverters, electrical spacers, or recharging stations, using aerial robotic manipulators [2] to reach quickly the power lines avoiding the risky conditions faced by human workers operating from manned helicopters or deployed on the power lines. These robots consist of a multi-rotor platform and suitable robotic arms with end effectors for each type of device [1]. The requirements and parameters associated with the manipulation operation, as represented in Figure 3-Middle, include the type

and number of devices to be installed, the separation distance between devices, the location and altitude of the installation point on the power line, and the required positioning accuracy and force (or lift load capacity) of the manipulator to conduct the installation operation.

Since the capabilities of aerial manipulators in free flight are limited due to wind perturbations and aerodynamic effects, it is convenient to land or perch on the line and then roll over it to perform the installations [26]. In this way, it is possible to increase the positioning accuracy and decrease the total operation time to install several devices. Two different approaches can be followed: 1) Integrated multi-functional platform able to fly, land or perch on the line, and roll over the line installing devices, and 2) Modular platform that can fly, deploy the manipulator on the line detaching it from the flying platform as in [23], and roll the manipulator over the line installing devices. In approach 2) the aerial platform may hover close to the robot or go back to the landing zone, landing to save energy and fly back to retrieve the manipulator after the installation of the devices.

The metrics of interest considered for evaluating the performance of the aerial manipulator in the installation of devices are the maximum number of devices that the robot can carry, the time required for perching on the power line from the take-off area, the time for landing from the installation point, the average time required to install each device, rolling speed when moving along the power line, and the maximum sag angle that the rolling base can overcome.

3.3 Aerial Co-Worker

The Aerial robotic Co-Worker (ACW) supports human operators in the realization of activities on the power lines, including voltage checks to ensure that the power line section is disconnected before other human operators access the workspace, the fast delivery of tools or devices when the operators are working at height on the line (see Figure 3-Right), and the visual tracking of the human workers to monitor safety.

The main requirements and parameters are: the specified contact point for checking the voltage of the power line; the time required by the field sensor to maintain contact with the power line for the voltage check; the location of the human worker with respect to the take-off position; the set of gestures or poses of the human workers that should be visually recognized by the aerial robot for the delivery operation; and the safety monitoring and other parameters relative to the operation (safety distance to humans, number of aerial robots and number of human operators to be monitored).

The metrics of interest for performance evaluation are: number of gestures and success rate in the visual recognition of gestures from the human operators; time required to conduct the voltage check (from take-off to landing); time required to deliver a device to the human worker on the line and maximum weight of the device being delivered; average reaction time of the multi-UAV system to the operator and human worker requests; and the ratio of mission time for which the human worker is visually tracked to check safety conditions.

It should be noted that even if the following sections consider specific methods and technologies, the above methodology is general for assessing the application of aerial robotics to I&M of electrical power lines.

4 Aerial Robotic Platforms

Figure 2 shows a selection of ten aerial robotic platforms developed or customized as part of the AERIAL-CORE project for the three aforementioned operation domains. Their main features are compared in Table 1. Although the number of developed platforms in AERIAL-CORE project was higher, we describe here only those that were evaluated in the final demonstration.

4.1 Long-Range Inspection Platforms

Five types of complementary aerial platforms were developed and evaluated in the long-range scenario including vertical take-off and landing (VTOL) UAVs and multirotors.

VTOLs combine the maneuverability of quadrotors with fixed-wing flight capabilities. A total of 3 VTOLs integrating visual and infrared cameras were used. Two of them (Marvin and Morpho) had morphing wings and can in-flight modify their characteristics. The third (DeltaQuad) was a commercial model capable of efficient and fast fixed-wing flight for fast and long-range visual inspection. Table 2 shows their main features. This is the first time that aerial platforms with morphing wings benefiting from adaptive aerodynamics are used for the inspection of a large linear infrastructure.

Two multi-rotor platforms were used for accurate and detailed inspection. One of them (Mapper) was equipped with 3D LiDAR, visual camera, and on-board processing resources and used for online semantic power line mapping. The second one (D-Ins) was designed for visual and infrared power line inspection and included autonomous vision-based landing on recharging stations. The main features of multi-rotor robots are shown in Table 3.

Table 2: Comparison of the particular features of the winged platforms for long-range inspection scenario.

Feature	Marvin	Morpho	DeltaQuad
VTOL capability	Yes	Yes	Yes
Wing morphing capability	Extension	Folding	No
Min. flight speed $[m/s]$	34	14	12
Max. flight speed $[m/s]$	-	20	28
Max. wind disturb. $[m/s]$	10	9	-
Wingspan $[m]$	1.85 - 2.41	0.54-1.8	2.35
Wing area $[m^2]$	0.53 - 0.71	0.35-0.54	0.9
Payload capacity $[kg]$	1	0.35	1.2
Max flight time $[min]$	60	17	90
Max flight range $[km]$	70	10	150

Table 3: Comparison of the particular features of the multi-rotor platforms used in the long-range inspection scenario.

Feature	Mapper	D-Ins
Type	Custom	Commercial
Platform	DJI M600	DJI M210
Max flight time $[min]$	15	24
Max flight range $[km]$	4	10
LiDAR sensor	Livox Horizon	-
Visual sensors	Intel RS D435i	Zenmuse H20T/XT2
Position sensor	DJI GPS	DJI RTK V2

These five platforms are described below.

4.1.1 Marvin

This industrial aerial platform adopts a VTOL configuration with tiltable rotors and morphing wings, as shown in Figure 4. It is based on a fixed-wing UAV structure combined with four rotors to achieve the VTOL capacity. It is improved by two mechanisms that allow to adjust

the wing orientation and its length/area so the platform can adapt its geometry to the different flight modes: smallest wingspan for VTOL and increased wingspan for lower flight speed and higher accuracy in the data capture. Marvin adapts its wingspan autonomously during the flight to meet the flight conditions, reducing the wing area to minimize the effect of wind perturbations. Its main features are presented in Table 2.

4.1.2 Morpho

This novel platform is a bioinspired, quad, morphing, biplane tailsitter VTOL that features four identical and independently actuated wings, combining the advantages of multi-rotors and fixed-wing UAVs in a single vehicle (see Figure 4). Morpho is capable of performing both hovering and long-range horizontal flight with autonomous way-point tracking. It can transform into a stable configuration with folded wings that will allow it to operate in vertical flight to capture detailed images of the infrastructure in close proximity. This prototype has been tested up to wind speeds of 9 m/s while maintaining its hovering position, demonstrating stable and lower energy consumption despite the gradual increase of the wind (see Figure 4-Right). The independent actuation of the wings improves energy efficiency and manoeuvrability in hovering flight [27], while the morphing capability allows Morpho to overcome the limitations for hovering and maintain stability under significant wind of current commercially available VTOL platforms with exposed wings [28]. Its main features are shown in Table 2. Morpho was validated in the ATLAS flight centre[5].

The wing-morphing control strategy of Morpho is built on top of the PX4 open-source cascaded architecture, integrating morphing wing actuation with differential thrust for enhanced position control. A custom controller manages differential morphing inputs to optimize stability and maneuverability in high winds. The control strategy leverages onboard IMU and airspeed sensors for adaptive response, ensuring real-time adjustments to aerodynamic loads. In particular, closed-loop controllers have been deployed for the wing morphing state when the wings are used for actively stabilizing yaw. The input is the yaw rate error computed by the flight controller and the output is the desired wing angle magnitude. The wing angle command is then sent to the servomotors, which track a trapezoidal velocity profile with a specific acceleration and a given top speed. As shown in [29], adaptive wing morphing while hovering in adverse wind conditions can reduce normalized energy consumption up to 85%, increase attitude and positional stability, and leverage wind energy to increase its yaw angular rate up to 200% while decreasing motor saturation levels, thus improving the system's operational capability and reliability.

4.1.3 DeltaQuad

It is a commercial UAV (DeltaQuad Pro), see Figure 2, a dual VTOL-fixed wing UAV combining quad-rotor flight mode for take-off and landing with fixed-wing mode for long-range inspection with RGB and infrared cameras. Its main specifications are collected in Table 2. The platform allows fully autonomous operation, from take-off, way-point navigation, to landing, thanks to a lightweight onboard computer with a customized software framework developed to integrate different autopilots [30]. The on-board camera is a Flir Duo Pro infrared camera.

4.1.4 Mapper

Based on the DJI Matrice 600 with BVLOS (beyond visual line of sight) flight capabilities, it was developed for power line online mapping and semantic segmentation in the long-range inspection scenario. It was customized by adding a Livox Horizon 3D solid-state LiDAR and

[5]Morpho flight experiments: `https://youtu.be/KfKCRcdeYYQ`

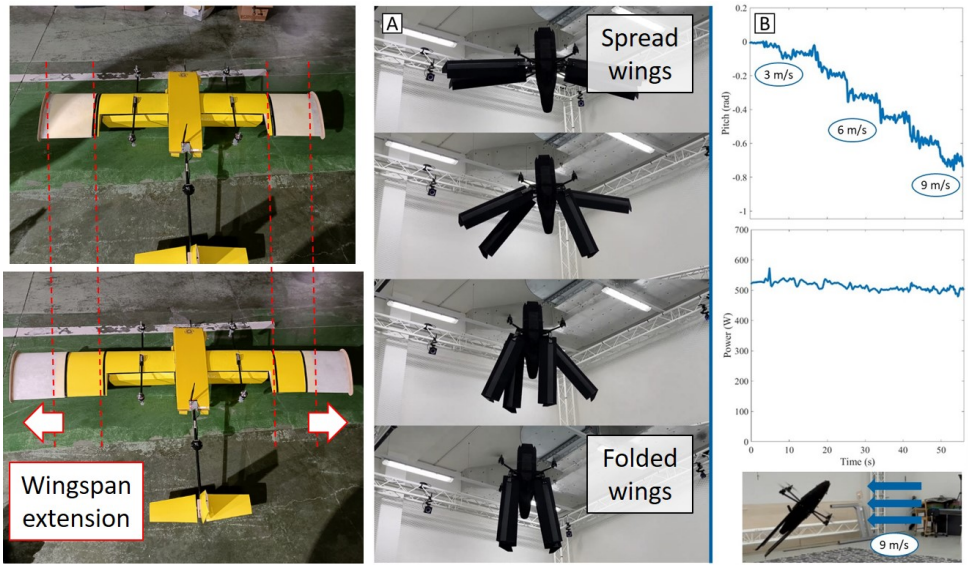

Figure 4: Left) Marvin-5 platform extending the wings. Center) Morpho in hovering flight with different wing configurations. Right) Morpho in hovering experiments, showing constant energy consumption for different wind speeds.

a Jetson NVIDIA NX Xavier computer board. It implemented online LiDAR-based mapping algorithms as well as LiDAR-based segmentation and classification of the environment in four classes: *Power Line*, *Towers*, *Soil*, and *Vegetation*. More than 80 experiments were conducted in BVLOS mission scenarios with different conditions and vegetation [13]. Figure 5-Bottom shows the map obtained online in the 3.7 km flight conducted as part of the final AERIAL-CORE demonstration.

4.1.5 D-Ins

A multi-rotor based on the DJI M210 platform used for detailed visual and infrared inspection of power lines and towers using the DJI Zenmuse cameras. The flight speed for inspection operations is limited to 20 km/h, with a maximum speed of 65 km/h, providing up to 30 min flight time. The platform incorporates a RTK-GPS for accurate positioning and navigation. It is endowed with onboard obstacle avoidance integrated within the mission planning framework developed for long-range inspection [30, 10]. The platforms also demonstrated the autonomous landing on recharging stations, see Figure 5-Top-Right.

4.2 Aerial Manipulation Platforms

The aerial manipulation platforms were specifically designed and developed to conduct the installation of devices on the power lines. Two platforms were evaluated: the Dual Arm Rolling Platform (DARP) for the installation of a customized model of clip-type bird flight diverter, and the Main Local Manipulation Platform (MLMP) for installing commercial bird flight diverters, electrical spacers, and recharging stations. Table 4 details the specifications of both platforms.

4.2.1 Dual Arm Rolling Platform (DARP)

Motivated by the benefits in energy efficiency, accuracy, and reliability of performing the manipulation operations in perching conditions instead of doing them while flying, the dual arm platform with rolling base shown in Figure 2 has been applied in the installation of a customized

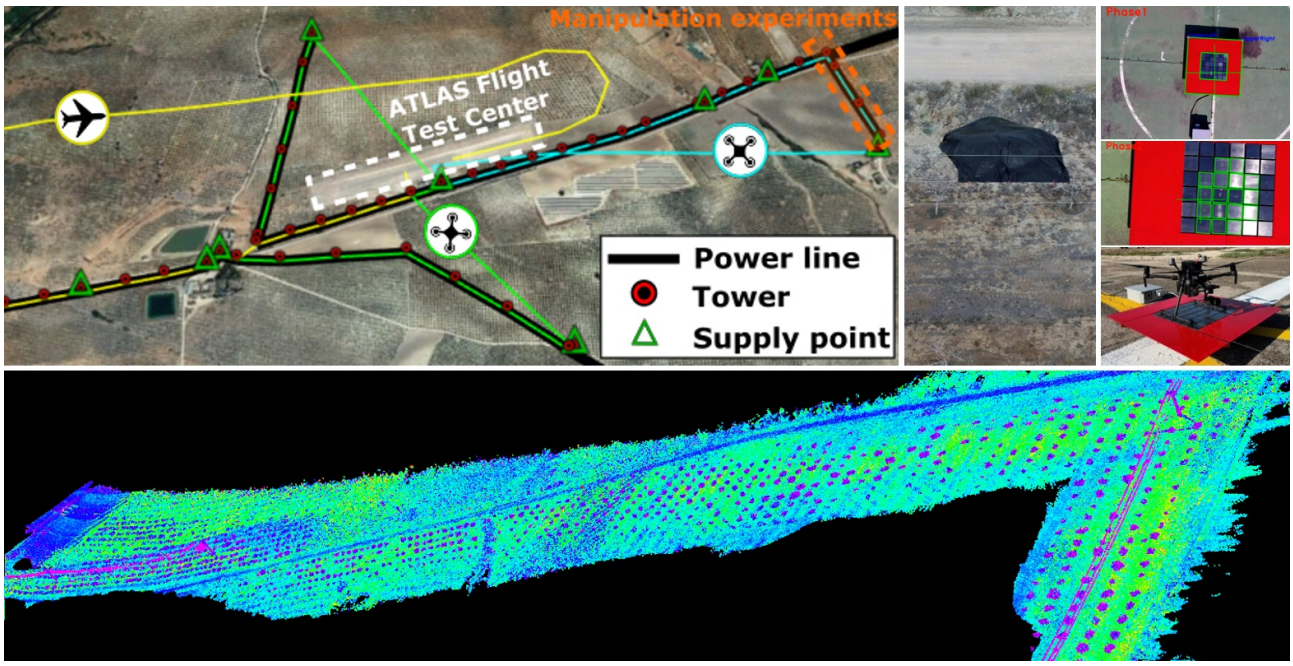

Figure 5: Top-left) Autonomous inspection of ATLAS power grid by multi-UAV team: planned trajectories. Top-center) A snapshot of the video streamed by one multi-rotor when a plastic foreign object hung from the line is detected. Top-right) Autonomous landing on charging station. Bottom) Resulting 3D map online computed by Mapper in the final AERIAL-CORE demonstration.

Table 4: Comparison of the features of the aerial manipulation robots.

Feature	DARP	MLMP
Manipulator	Dual arm	Single arm
Arm DOFs	2×4	6
Arm payload $[kg]$	0.5	3
Capacity $[devices]$	4	1
Install diverters	Yes, custom	Yes, standard
Install spacers	No	Yes, standard
Install recharg stat.	No	Yes, prototype
Aerial platform	Custom	Prototype
Perching mode	From above	From below
Rolling speed $[m/s]$	0.15	0.5
Weight $[kg]$	3.5 + 4.5	45
Flight time $[min]$	10	17
LiPo battery $[mAh]$	$2 \times$ 4,500 6S	$2 \times$ 6S 22,000

model of bird flight diverters on real power lines. The robot consists of a lightweight and compliant anthropomorphic dual-arm system LiCAS A1 (3 kg weight, 0.5 kg payload) equipped with a servo-driven rolling base (0.15 m/s speed) and magnetic grippers for grasping the devices placed in a double array [23]. The dual arm manipulator is transported, deployed on the line, and retrieved by the carrier multi-rotor using a hook-handle mechanism. The platform is a quadrotor based on the Tarot X4 frame with RTK-GPS for controlling the position and trajectory of the platform, and a Cube Black autopilot running the ArduPilot flight controller. The control program of the arms, developed in C/C++, runs onboard on a Raspberry Pi 3 and includes a specific task for autonomous installation of the devices, executed as a sequence of

Cartesian way-points for both end effectors.

4.2.2 Main Local Manipulation Platform (MLMP)

This aerial robot can fly to the line and detect the line, perch autonomously on the line, and install or uninstall various devices as it moves along the cable [31]. The robot has been designed and tested to operate with charged power lines of up to 125 kV. Its grounded metal frame serves as a Faraday cage by protecting electronic components from electromagnetic interference while absorbing voltage arcs produced by the power line. The specially designed perching mechanism enables the system to perform the perching manoeuvre and to move along the power line by means of its integrated pulleys connected to DC motors. Additionally, the frame can integrate various tools and devices, such as the robotic arm that performs the manipulation. With a maximum take-off weight (MTOW) of 45 kg, MLMP is capable of flying for 17 minutes, enough time to perform up to 5 perching manoeuvres or a complete multi-device installation operation on a power line.

It should be noted that no other autonomous aerial manipulators have demonstrated efficient installation of multiple devices on power lines, including energized ones, thanks to the combined capability of flying and rolling over conductors (DARP and MLMP), including deployment and retrieval of the manipulator (DARP). In addition, to date, no other aerial manipulator has been applied to the installation of several types of devices on the power lines (MLMP).

4.3 Aerial Co-Working Platforms

Three multi-rotor platforms have been developed and tested to assist human operators (see Figure 2), working on power lines, addressing three use cases: voltage check to determine if a line section was correctly disconnected from the grid before human intervention; tool delivery to human operators working on power lines; and monitoring safety conditions of human operators working on the power lines.

4.3.1 ACW-V, ACW-D

The aerial co-worker robot consists of a hexarotor with fixed-tilted rotors, enabling full actuation and thus a precise, independent control of both position and orientation, which is key when working close to humans. The platform integrates a 3D LiDAR, allowing accurate navigation with a previously generated map. The platform size (tip-to-tip distance of 1 m) and weight (3 kg without payload) are appropriate to operate in close proximity with human workers. It has been validated in two applications within the AERIAL-CORE system (see Section 7): voltage check (ACW-V), and tool delivery (ACW-D). ACW-V includes a rod with a frame to touch the cable and detect if the power line is live. ACW-D has a delivery system consisting of a pulley and clamp mechanism. An RGB-D camera and a Jetson AGX Xavier onboard computer were integrated to implement the gesture recognition methods [32].

4.3.2 Safe-CW

These multi-rotor platforms are designed to monitor human operators during power line I&M tasks while being able to offer the operator detailed additional views of the power line infrastructure. The developed robot is based on the Holybro X500 frame, with a maximum take-off weight (MTOW) of 3.5 kg. It is equipped with a downwards and upwards-oriented depth camera and a 3D LiDAR for obstacle detection and human operator localization, using RTK-GPS for positioning, and a front-facing RGB camera for power line inspection and monitoring the operator during the work.

Compared with existing works, there is no aerial co-working platform that has been demonstrated previously in the maintenance of the electrical power systems.

5 Long-Range Inspection Methods and Results

This section describes the main functionalities implemented for conducting autonomous visual and LiDAR-based long-range inspection of a power grid area, presenting results from the experimental evaluation of the platforms introduced in Section 4.1 following the metrics defined in Section 3.1.

5.1 Tracking

In AERIAL-CORE, we have developed an RGB-based [12] and an event-based [33] power line trackers, as depicted in Figure 6. The RGB-based power line tracker [12] is a novel algorithm that extends the deep-learning–based object detector in [34] to the case of power line detection. The perception module is trained on synthetic data only and transfers zero-shot to real-world images of power lines without fine-tuning. In this way, the problem of the limited amount of annotated data for supervised learning is overcome. The detector takes a single RGB image as input and outputs end points of the detected power lines in pixel coordinates. The center patch of each detection is matched with the prediction of the previous patch using the Hungarian method. We use a KLT tracker [35] to perform tracking. To train the detector, a new synthetic dataset for power line detection based on a simulator was generated. The model was then trained on 30k simulated images, demonstrating real-world deployment without fine-tuning on real images. Table 5 includes a quantitative evaluation of the performance of the RGB power line tracker and of the classical approaches using the metrics proposed in [36] (P: Precision, R: Recall, F: F1 Score). Our proposed method outperforms the classical approaches in all the metrics and it is computationally efficient to be run on the computer onboard the drone. Run Time refers to the time required to process a single image on the Nvidia Jetson TX2.

Table 6 includes a comparison of the state-of-the-art line detection methods with respect to their inference speeds. Our approach outperforms the state-of-the-art methods in terms of computational efficiency. The methods [37, 38, 39, 40, 41] have a too large run time to be included in our closed-loop controller system. All experiments use the same input image size of 512 × 512 on Nvidia GeForce RTX 2080Ti GPU. The event-based line tracking method [33] is compared against the event-based line tracking method proposed in [42] onboard the drone. Our method can track the visible power lines for an average time of 31.12 [s]. This time is 10 times longer than the average tracking time achieved by [42].

Table 5: A quantitative evaluation of the performance of the RGB learning-based line detector.

Method	**Chamfer Distance**			**EA Score**			**Run Time [ms]**
	P	R	F	P	R	F	
Hough Transform	0.70	0.32	0.44	0.46	0.19	0.28	18.52
P-Hough Transform	0.26	0.31	0.28	0.10	0.16	0.10	**16.13**
Ours	**0.92**	**0.77**	**0.84**	**0.93**	**0.78**	**0.85**	20.83
Improvement [%]	31	141	91	102	311	204	–

Event cameras [43] are inherently robust to motion blur and have low latency and high dynamic range. Thus, they are advantageous for the autonomous inspection of power lines

Table 6: Comparison of the state-of-the-art line detection methods with respect to their inference speeds.

Method	**Run Time [ms]**
SCNN [37]	133.33
LaneATT [38]	38.46
CondLane [39]	17.18
Line-CNN [40]	27.93
PointLaneNet [41]	14.08
Ours	**1.80**

with UAVs, where fast motions and challenging lighting conditions are ordinary. Our event-based power line tracker [33] identifies lines in the stream of events by detecting planes in the spatio-temporal signal and tracking them through the time. The algorithm can persistently track autonomously the power lines, with a mean lifetime of the line 10 times longer than existing approaches [42]. Both methods were validated onboard a quadrotor equipped with an Nvidia Jetson TX2 [44].

Figure 6: Left) output of the event-based tracker [33]. The algorithm assigns to each tracked line a unique ID. Right) output of the RGB-based tracker [12]. The algorithm assigns to each tracked line its inclination (positive or negative), a confidence score, and a unique ID (not visualized).

The planning and control method used onboard the quadrotors for approaching and following power lines is based on a perception-aware MPC algorithm [45, 11], specifically adapted to incorporate power line tracking as an objective in the optimization problem [12]. The proposed MPC algorithm plans and tracks a trajectory that maximizes the visibility of the power line in the onboard camera view while ensuring safe avoidance of obstacles such as power masts. It includes two perception objectives: one for line tracking and another for collision avoidance, with their respective weights optimized online. The details of this approach are presented in [12].

5.2 Long-Range Mapping

Mandatory power line inspection includes the detection of violations of safety distances between the power line and electric transmission towers, and the surrounding vegetation. The traditional

approach is based on capturing images and LiDAR data using manned helicopters and off-processing them in the office to obtain (weeks later) the resulting segmented map, which is very inefficient and leads to repetitions of data gathering flights. In AERIAL-CORE, an online LiDAR-based 3D semantic mapping system for UAV long-range power-line inspection has been developed. The method implemented onboard the Mapper platform (see Section 4.1) is based on *FAST-LIO2*. To deal with scenarios with a lack of geometrical features, we integrated GNSS measurements within *FAST-LIO2*. The measurement model is obtained by estimating the position of the GNSS receiver at the current instant given the state of the robot: $h\left(\mathbf{x}, \boldsymbol{\nu}\right) = \mathbf{T}_G^W \mathbf{T}_W^I \left(\mathbf{p}_I + \boldsymbol{\nu}_I\right)$, where $\mathbf{x}$ is the state of the robot, that includes $\mathbf{T}_G^W = \{\mathbf{t}_G^W, \mathbf{R}_G^W\}$ and $\mathbf{T}_W^I = \{\mathbf{t}_W^I, \mathbf{R}_W^I\}$, which are the transformations between the GNSS frame G and the global map frame W, and between W and the current inertial frame of the robot I. Also, $\mathbf{p}_I$ is the position of the GNSS sensor in the inertial frame of the robot (assumed fixed and calibrated with precision), and $\boldsymbol{\nu}_I \sim \mathcal{N}\left(\mathbf{0}, \mathcal{Q}_{\text{GNSS}}\right)$ models the uncertainty of the measurement. This measurement model can be simply subtracted to $\mathbf{z}_G$ (the measured position in the GNSS frame) to obtain the residual required for the error-state manifold-based iterative Kalman Filter (*IKFoM*) of *FAST-LIO2*. In addition to this residual, the implementation of the GNSS inside the *IKFoM* requires the derivation of two Jacobians [46]. Taking the full state vector as $\mathbf{x} = \{\mathbf{t}_W^I, \mathbf{R}_W^I\, \mathbf{t}_G^W, \mathbf{R}_G^W\ \}$, the Jacobians are computed as:

$$\mathbf{H} = \left.\frac{\partial h\left(\mathbf{x} \boxplus \delta\mathbf{x}, \mathbf{0}\right)}{\partial \delta\mathbf{x}}\right|_{\delta\mathbf{x}=\mathbf{0}} \in \mathbb{R}^{3\times 12} = \begin{bmatrix}\mathbf{R}_G^W & -\mathbf{R}_G^W \mathbf{R}_W^I \lfloor \mathbf{p}_I \rfloor & \mathbf{I}_3 & -\mathbf{R}_G^W \lfloor \mathbf{T}_W^I \mathbf{p}_I \rfloor\end{bmatrix} \tag{1}$$

$$\mathbf{D} = \left.\frac{\partial\left(\mathbf{x}, \boldsymbol{\nu}\right)}{\partial \boldsymbol{\nu}}\right|_{\delta\boldsymbol{\nu}=\mathbf{0}} = \mathbf{R}_G^W \mathbf{R}_W^I \in \mathbb{R}^{3\times 3} \tag{2}$$

With these Jacobians, the covariance of the measurement model is projected into the reference frame G of the GNSS measurements as $\bar{\mathcal{Q}}_{\text{GNSS}} = \mathbf{D}\mathcal{Q}_{\text{GNSS}}\mathbf{D}^T$, which is the value finally used in the *IKFoM*. We define directly $\bar{\mathcal{Q}}_{\text{GNSS}}$ instead of $\mathcal{Q}_{\text{GNSS}}$, since it is given in the reference frame G, which is in general aligned with the horizontal and vertical axis, that have covariance estimations typically made available by the GNSS manufacturer. Finally, the transformation from G to W has to be given an initial guess and an initial confidence level (covariance). We measured the translation and rotation values of that transformation manually, but gave null confidence to the yaw-axis rotation between them, so the initial angle to the north of the GNSS system can be estimated automatically by the mapping module.

The accuracy of the mapping method was evaluated in preliminary experiments performed in the ETSI Outdoor Flight Testbed of the University of Seville by analyzing the errors w.r.t. a millimeter-accuracy ground-truth map obtained with a Leica Nova MS60 total station. Figure 7 shows the map generated in real time onboard the Mapper platform overlapped with the ground-truth map (left) and the resulting mapping error histogram (right). The fashion (most probable value) of the error histogram is 5 cm, while the mean mapping error value is 7.2 cm.

The mapping method was enhanced with LiDAR-based segmentation that classifies the map point cloud into *Power Lines*, *Towers*, *Vegetation*, and *Soil* by combining LiDAR reflectivity region growing (to differentiate between metallic and non-metallic objects) and Principal Component Analysis (to consider the point-cloud spatial distribution) [47]. Figure 5 shows the segmented 3D map obtained of the power grid area covered in the final AERIAL-CORE demonstration in a flight of >3.7 km. The results from the semantic classification according to the metrics defined in Section 3.1, shown in Table 7, largely overtake existing methods such as *PointNet++* [48].

No other fully autonomous aerial robotic system has demonstrated long-range mapping of the power line elements and surrounding vegetation with on-line onboard execution so far.

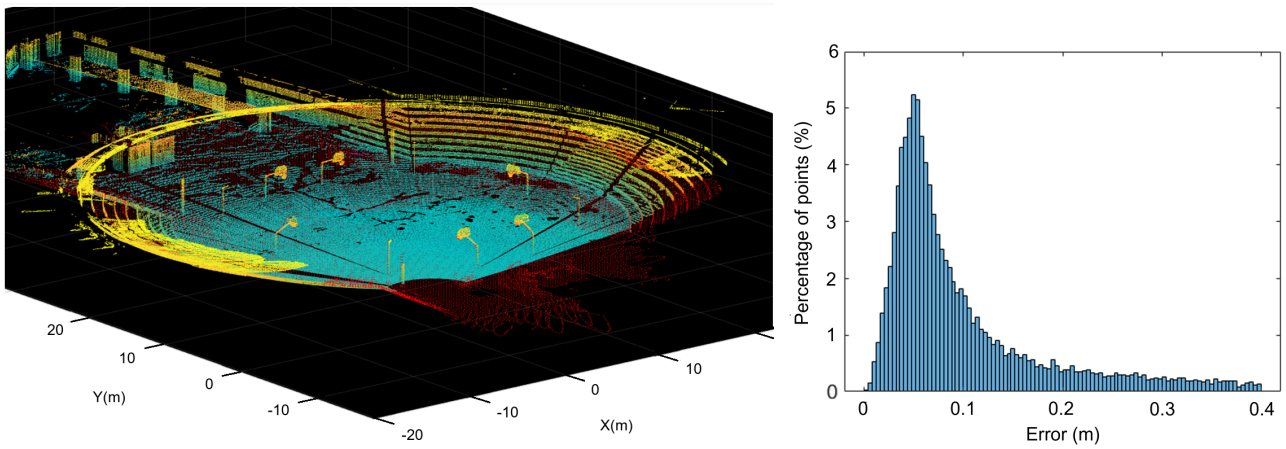

Figure 7: Validation of the AERIAL-CORE mapping method: Left) map generated online on board by Mapper multirotor overlapped with the millimeter-accuracy ground-truth map built with a Leica Nova MS60 total station, Right) resulting mapping error histogram.

Table 7: Results of the LiDAR-based semantic classification obtained with Mapper platform and comparison versus *PointNet++* [48] in all the performed experiments.

Metric	Precision(%)		Recall(%)		F_1 score(%)	
	Ours	[48]	*Ours*	[48]	*Ours*	[48]
Power line	96.23	**100.0**	**96.51**	77.78	**96.36**	87.50
Tower	**84.95**	41.48	**86.72**	50.33	**85.82**	45.48
Vegetation	**99.63**	99.27	98.89	**99.86**	99.26	**99.57**
Soil	98.01	**99.95**	**99.84**	99.72	98.92	**99.83**

5.3 Multi-UAV Inspection with Autonomous Landing

When powerful storms hit an area, they usually cause foreign objects like trees and large plastic fabrics, falling to power lines and generating power outages. In this context, it is crucial to minimize the time needed to find the outage location and reestablish the power supply. To cope with that, AERIAL-CORE has developed a heterogeneous multi-UAV inspection system with cognitive capabilities, involving three of the platforms described in Section 4.1: multirotor D-Ins, DeltaQuad, and tiltable morphing-wing VTOL Marvin, which were endowed with autonomous navigation capability and equipped with high-resolution cameras to capture and stream information from the environment.

A planning method for autonomous cooperative inspection of electric power grids was developed to achieve safe and efficient multi-UAV operation [10, 30], minimizing the total inspection time. It exploits the heterogeneous capabilities of the fleet and integrates terrain models for safe and accurate positioning and energy consumption models based on the UAV aerodynamics (including the wind effect and other weather conditions) to predict the optimal time to recharge the batteries. Moreover, due to the limited battery capacity of the UAVs, charging stations deployed along the operation area were also considered in the planner to enable long-endurance operations. Whenever a UAV needs to land at a charging station, it uses visual servoing to enable accurate autonomous landing, see Figure 5-Top right. This novel multi-UAV planning method for the inspection of power lines has been developed for the first time for a cooperative team of heterogeneous aerial robots, dealing with the integration of the planner with the UAV fleet, the fulfillment of end-users' requirements, and other practical aspects related to the real field deployment (including avoiding collision with the power line cables and towers). Other state-of-the-art approaches usually consider only one UAV, or prioritise the formulation of the-

oretical problems and their solution methods without thoroughly evaluating the effectiveness of the resulting plans during real-world UAV inspections. Thus, many of them focus on solving large grids, sometimes artificially complex, in bounded computation times. However, they are at the same time disregarding practical aspects such as current regulatory restrictions, the effect of weather conditions, the variation of energy consumption with the wind on planned routes, or the requirements imposed by end users to guarantee a certain level of quality in captured images or videos.

The problem of inspection of an electrical power grid by means of an aerial multi-robot inspection team can be modelled using a directed weighted multigraph $\mathscr{G} = (\mathscr{V}, \mathscr{E}, \mathscr{W}, \mathscr{D})$, where $\mathscr{V}$ represents the nodes $\mathscr{V} = \mathscr{P} \cup \mathscr{O}$, which consist of two components, the set $\mathscr{P}$ of n towers and the set $\mathscr{O}$ of m base stations of the aerial robots, $\mathscr{E}$ are the edges that connect the nodes representing aerial robot paths, $\mathscr{W} = \mathscr{T} \cup \mathscr{B}$ where the sets $\mathscr{T}$ and $\mathscr{B}$ are the cost in term of flight time and battery consumption respectively, and $\mathscr{D}$ are the m active robots in the team. The inspection mission can be formulated as the minimization of the inspection time T of all the edges associated with power-line segments, taking into account that each UAV should start and finish in its base station, and the battery consumption constraints which depend on the particular UAV and the direction of the path which should be selected depending on the wind direction.

Optimizing the mission duration for the multi-robot team requires minimizing the inspection time of the aerial robot that takes the longest time to complete its route [10], as the mission concludes only once the last aerial robot has returned to its station. The problem is a "capacitated min-max multi-depot VRP (Vehicle Routing Problem)", and its exact solution can be obtained using Mixed Integer Linear Programming reformulated to minimize the sum of all inspection times for all UAVs, while aiming to keep these times balanced. The computational efficiency can be improved using a clustering method that groups segments of the power grid located within the same branches based on a consumption criterion, creating simplified branches that represent the original ones.

Particular attention has been paid to determine the above-mentioned constraints due to aerial robot battery consumption in contrast to other simplified models used for planning purposes [10]. Thus, based on the blade momentum theory and conservation of energy, we have obtained more accurate estimations of energy consumption of multi-rotors and VTOLs by computing the aerodynamic power given by three terms: the induced power to speed up the rotor airflow and produce thrust, the drag of the rotor blades, and the parasitic power required to counteract the drag of the airframe. We have validated experimentally the estimations for different payloads and different wind conditions.

The long-range UAV fleet was evaluated in the power grid area around the ATLAS Flight Center (see Figure 5-Top left), demonstrating their capability to autonomously inspect 10 km of power lines in 10 minutes according to the end-users' requirements. During this particular inspection, the time required to detect and localize the failure (plastic fabric) tangled in the power-line cables was 6 min. In contrast, the local maintenance supplier estimates that human inspectors would require approximately 30 minutes to fully inspect the same power grid under ideal conditions, where both personnel and vehicles are readily available. Consequently, the multi-UAV approach reduces the total inspection time by about 66%. The time required to compute the mission plan in the multi-UAV system was 7 s. The GSD of the visual images provided by the detailed inspection multi-rotor (D-Ins) was 2 mm, whereas the GSD obtained with the tiltable morphing-wing VTOL was 3 mm. It should be mentioned that an average wind speed of 10.08 km/h was measured in the operation area at the time of the demonstration, which did not significantly affect the quality of the results.

The previous planning results were compared with those obtained using a formulation of the well-known Travelling Salesman Problem (TSP) [49]. This formulation was adapted to

address multi-tour, single-depot scenarios, where the inspection mission can be distributed among multiple UAVs to accelerate the operation, particularly in cases where a single UAV flight time is insufficient to complete the inspection in one tour. The results obtained from the TSP-based approach yield longer overall mission times compared to those achieved with the method proposed in this paper. Specifically, our approach demonstrated a 29.81% reduction in the total time required to plan and execute the mission. It is also worth highlighting that this and other state-of-the-art methods lack several key features integrated into our approach. Notably, our method incorporates path adaptation to maintain an optimal video perspective and includes a precise battery consumption model, both of which have proven essential for the practical and efficient execution of real-world inspection tasks.

6 Aerial Manipulation for Maintenance: Methods and Results

This section presents the functionalities, experimental results, and validation of the two aerial manipulation robots from Section 4.2 devoted to the installation of devices on power lines. The experiments were conducted in a real power line, at 10 m height, close to the ATLAS Flight Center.

6.1 Installation of bird diverters with the DARP platform

6.1.1 System Modeling

A model of the aerial deployment and retrieval operation carried out by the DARP is derived here to better understand the involved physical effects. Four reference frames are defined in the first place, as depicted in Figure 8: the World fixed frame $\{\mathbf{W}\}$ associated to the take-off and landing position, the multi-rotor base frame $\{\mathbf{B}\}$ located at the center of mass (CoM) of the platform, the hook reference frame $\{\mathbf{H}\}$ considered only for the dual arm retrieval phase, and the dual arm frame $\{\mathbf{A}\}$ located at the midpoint of both left and right arms, with the X-axis pointing forwards, the Y-axis parallel to the shoulder axis, and the Z-axis pointing upwards.

The position and orientation of the multi-rotor platform w.r.t. $\{\mathbf{W}\}$, given by the on-board positioning system, will be denoted by $\mathbf{r}_{\mathbf{B}}^{\mathbf{W}} \in \mathbb{R}^3$ and $\eta_{\mathbf{B}}^{\mathbf{W}} \in \mathbb{R}^3$, respectively, using Euler angles for the orientation. The kinematics and dynamics of the anthropomorphic compliant dual arm can be found in [50], comprising upper arm and forearm link lengths (L_1 and L_2) and the separation between both arms (D). Now, the derivation of the kinematics and dynamics of the system will be different according to each of the two phases. On the one hand, in the deployment phase, the hook-handle mechanism introduces a passive joint, denoted as q_0, which makes the arms tilt in the pitch angle w.r.t. the multi-rotor base frame. When the arms are deployed in the line, they are detached from the multi-rotor due to the action of the preloaded spring that releases the hook from the handle once the rolling base lays on the power line [23]. In that moment, the aerial platform and the dual arm become physically independent systems. On the other hand, the cable-suspended hook used to retrieve the arms by the handle is tied to the multi-rotor base by a couple of elastic cables of natural length L_0 separated a distance D_c. Cables are characterized by their mass m_c, axial stiffness k_c^a and damping d_c^a, bending stiffness k_c^b and damping d_c^b. These last two parameters are relevant in practice to prevent excessive oscillation of the cables during the retrieval phase due to the perturbation induced by the wind over the suspended hook. The motion of the hook w.r.t. the multi-rotor base can be approximated by a Cartesian displacement $\Delta\mathbf{r}_h^{\mathbf{B}} = [\Delta x, \Delta y, \Delta z]$ and a torsion angle $\Delta\psi_h^{\mathbf{B}}$ in yaw, assuming that the hook remains approximately parallel to the ground plane during the

retrieval phase due to its own weight. This arrangement can be assimilated to an elastic slung load [51] or a macro-mini aerial manipulator with elastic suspension [52].

The remaining physical parameters involved in the model are the mass m_B and inertia tensor of the multi-rotor, the mass m_A and inertia parameters of the dual arm [23], the mass m_c of the cables (the linear mass density varies with the elongation) and the mass m_h of the hook, which should be considered in the pre-capture phase, but it becomes negligible once the dual arm is retrieved. The dynamic model of a cable suspended dual arm aerial manipulator for the case of purely stiff cables is presented in our previous work [53]. The hook mechanism can be approximated by a rectangular surface affected by the aerodynamic drag force $\mathbf{F}_A^h = C_d^h \mathbf{v}_w$ due to wind vector $\mathbf{v}_w$. This force will depend on the aerodynamic drag coefficient C_d^h, determined by the geometry of the hook, assuming turbulent flow. When suspended from the aerial platform, the motion of the hook is determined by three forces: (1) the ones exerted by the cables, (2) the aerodynamic drag due to the friction with the air, and (3) the load exerted when the dual arm is retrieved, considering the cable elongation $\Delta L = -\Delta z$.

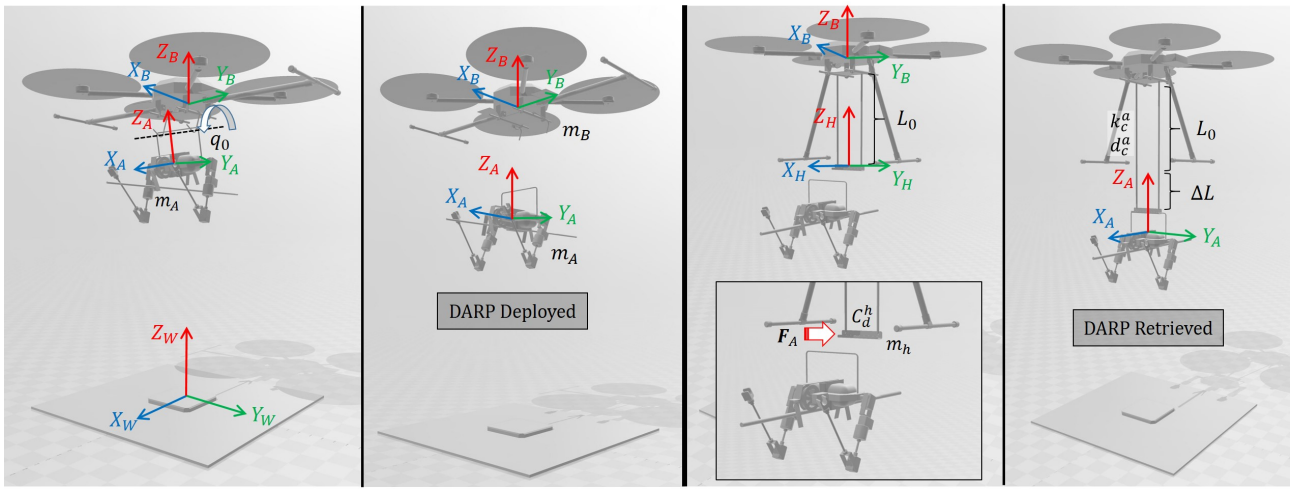

Figure 8: Reference frames and physical parameters considered in the kinematic and dynamic model of the DARP during the aerial deployment (left) and retrieval (right) phases.

Three main effects having a noticeable effect were identified during the experimental testing, which are related to the deployment and retrieval model described above:

- When the dual arm is deployed on the line, there is a sudden loss in the mass of the aerial platform from $m_B + m_A$ to m_B (which is around 30% loss), so the altitude controller will exert momentarily an excessive thrust with the consequent altitude increase until the controller is adapted to the new weight.

- The aerodynamic wrenches exerted on the hook due to the wind and the downwash coming from the propellers can be modeled as a force/torque perturbation exerted over the hook surface. To overcome their effect, it is convenient to increase the stiffness and damping of the cables.

- The elasticity of the cable pair used to suspend the hook from the multi-rotor base provides a smooth and passive accommodation of the multi-rotor altitude controller when the dual arm is retrieved.

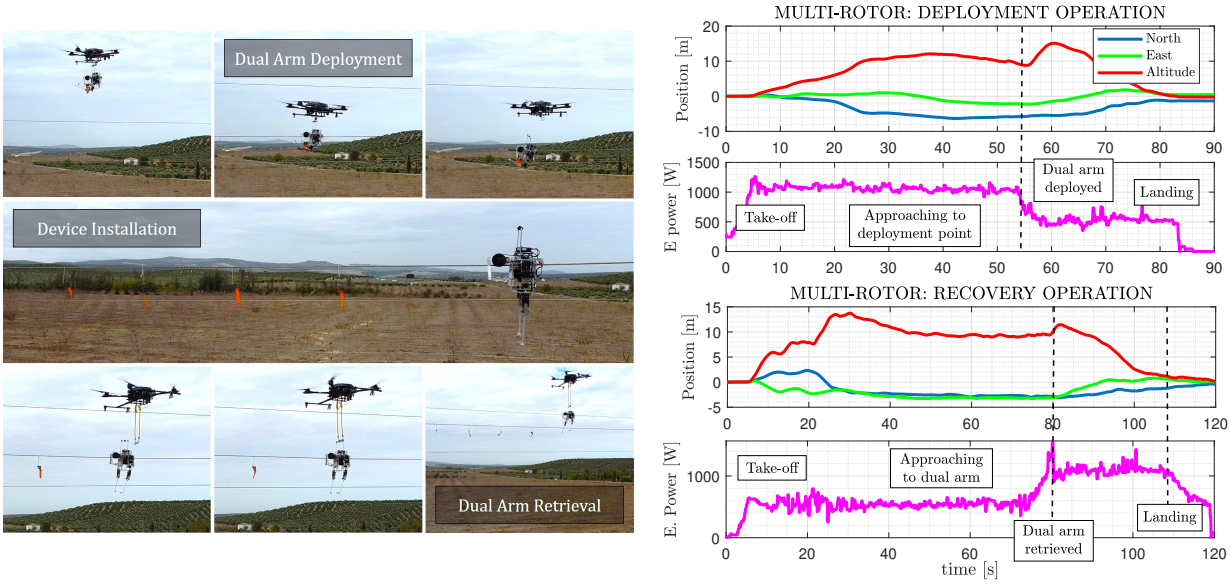

Figure 9: Validation of the DARP on a real power line for the installation of customized clip-type bird diverters in the ATLAS flight center: sequence of images from video (left), aerial deployment and retrieval (right) phases.

6.1.2 System Validation

DARP was validated[6] through the installation of four bird-flight diverters in one of the three cables of the power line section. The installation operation, shown in Figure 9, comprises three phases: 1) the aerial deployment of the dual arm robot on the power line using the multi-rotor, which is detached when a preloaded hook-handle mechanism is released once the arms are supported on the line [23]; 2) the installation of the devices carried by the manipulator; and 3) the aerial retrieval using a double cable suspended magnetic hook mechanism. The resulting performance according to the metrics defined in Section 3.2 is shown in Table 8. The arms provide a positioning accuracy at end effector lower than 5 mm, with a success rate in the installation of devices higher than 90%, taking into account the tests conducted on a ground power line mockup testbed. Figure 9 shows the electric power consumption of the multi-rotor, changing from 500 to 1000 W when the dual arm is attached. Stable perching of the arms is achieved since the center of mass of the dual arm system is ∼5 cm below the cable that supports the rolling base, similar to a pendulum. The device installation operation is programmed as a sequence of way-points for both end effectors, detaching the device from the magnetic gripper by generating an impulsive motion against the cable, relying on the mechanical joint compliance of the arms to support the physical interaction [23]. The DARP installed the four devices carried in the left and right arrays in 60 seconds, maintaining a separation distance of 85 cm between them. The robot rolls along the line at an average speed of 12 cm/s for 25 seconds in total, dedicating 35 seconds to the installation of the four devices. Since the weight of the dual arm robot deployed on the line is low (3 kg) the deflection caused on the line (sag, Δs in Figure 3) is small, less than 10 cm, as confirmed by visual inspection from the video sequence.

The deployment of the DARP on the power line was conditioned by weather conditions. A subsequent experiment was conducted during the same validation campaign under adverse conditions, including sporadic rain and wind. On that occasion, the drive wheel of the dual arm was not properly aligned with the cable during the deployment phase due to the oscillations induced by the wind. Since the robot was not able to roll along the line, it had to be retrieved

[6]DARP Video: https://www.youtube.com/watch?v=I8Ou9y5vrc0

Table 8: Experimental results from DARP and MLMP.

Metrics	DARP	MLMP
Devices installed	4	4
Distance bw. devices $[m]$	1.5	-
Deployment time $[s]$	80	120
Device install. time $[s]$	15	250
Go back land time $[s]$	90	300
Sag increment (Δs, $[m]$)	< 0.1	> 0.5

after installing a single device, using the teleoperation interface described in [54] to overcome the deviation in the pose of the arms. The expert human pilot responsible of the multi-rotor recommended not flying at wind speeds above 10-15 km/h, completely ruling out flying at speeds above 30 km/h. The retrieval phase also becomes more challenging as the wind speed is higher, since the aerodynamic drag acting on the cable-suspended hook tends to increase the amplitude of the oscillations, degrading the positioning accuracy required to retrieve the dual arm.

6.2 Installation of devices with the MLMP platform

MLMP has been validated, as depicted in Figure 10, via the installation and removal of commercial clip-type bird diverters and a prototype of charging station, (see Section 6.3) on a real power line. The performance obtained in these experiments is indicated in Table 8. The MLMP is capable of autonomously perching on a power line, moving along it, and manipulating devices with a robotic arm.

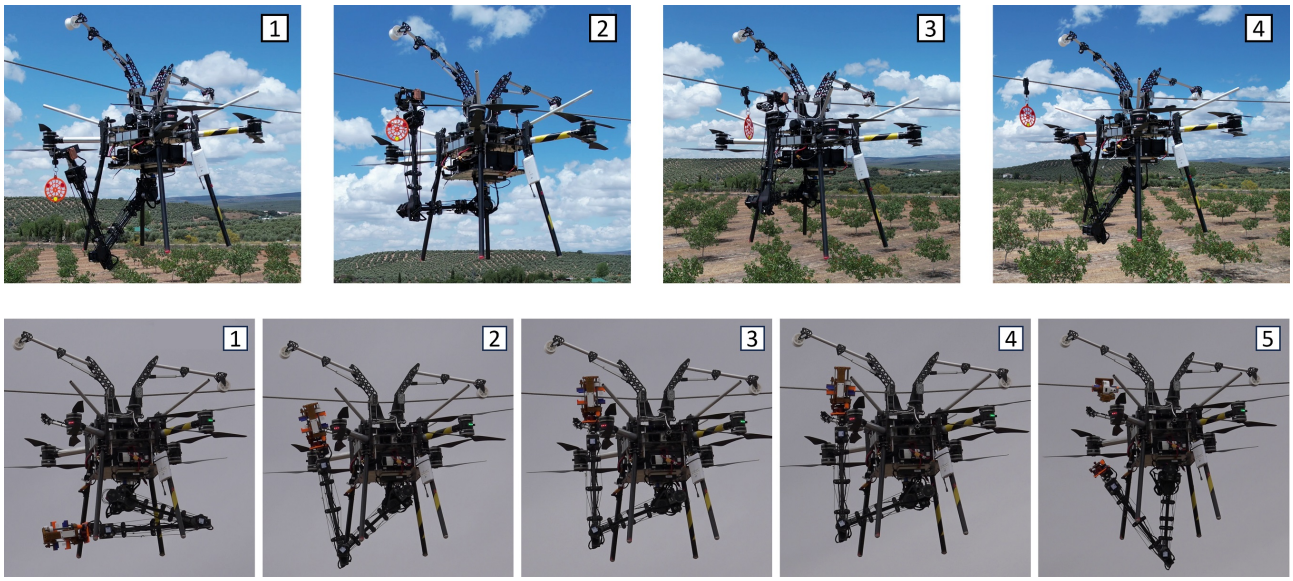

Figure 10: Installation of clip-type bird diverter (top) and recharging station (bottom) carried out by the MLMP. The installation of the devices begins with the MLMP perching on the power line and the robotic arm in a retracted pose (photo 1 bottom). The device carried by the end effector is approached to the installation point on the power line (photo 1 top and photo 2 bottom). Then, the device is installed on the cable by actuating the end effector (photo 2 top, photos 3 and 4 bottom). Once the device is attached to the line, the robot arm moves back to the retracted position (photos 3 and 4 top, photo 5 bottom).

The robotic arm of MLMP, designed specifically for high payload manipulation, is an anthro-

pomorphic arm featuring six degrees of freedom, with a gear-based spherical wrist to achieve enhanced dexterity and enable the arm to accomplish all designated tasks [55]. It provides 5 kg payload capacity while weighing only 3 kg, featuring a remarkable payload/weight ratio of 1.67, which sets it apart from other existing solutions. Specific end effectors were designed for the installation/deinstallation of clip-type bird diverters and the charging station. The first end effector simply pushes the bird diverter mechanism until it closes (see Figure 11-Top left). The end effector for the charging station was developed together with the charging station [56], see Figure 11-Bottom left. This end effector holds the charging station securely in place during transportation to the power line. The charging station is attached to the power line and released from the end effector by actuating it. The velocity of the end effector of the arm of the MLMP is 5.20 cm/sec. The time for the installation of a clip-type bird diverter with this arm is 14 sec. As indicated in Table 8, the installation of a single device with the MLMP is around 250 s. Although the installation time compared to the DARP is significantly higher, it should be noted that the MLMP was specifically designed to install standard devices currently used in the Spanish power grid, whereas the DARP employs a custom made device developed to simplify the installation process.

6.3 Charging Stations and their Installation

The magnetic field generated by the power line is the energy source for the developed charging stations, allowing drones to recharge while inspecting high-voltage power lines. A lightweight charging station (2 kg weight) has been developed and integrated into the MLMP for installation, as depicted in Figure 11-Bottom. The station incorporates a split-core current transformer for energy harvesting and an electronic circuit to convert the harvested energy to DC for recharging the station's battery. Further optimization of the design is achieved through the integration of the transfer window alignment method with the perturb and observe algorithm and a silicon steel core [57]. Experimental results revealed a significant 58.6% increase in harvested power compared to traditional methods. Notably, our proposed approach allows the charging circuit to automatically identify the maximum power point, regardless of fluctuations in the current on the power lines, eliminating the need to sense the primary current.

6.4 Teleoperation System

In addition to the autonomous installation of devices developed as part of the MLMP system, a teleoperation system was implemented to extend the range of operations that MLMP can conduct, taking benefit of the manipulation skills of the human operators. The IMU-based teleoperation method for the robotic arm [1] of MLMP was validated under realistic conditions for installing clip-type bird diverters, see Figure 11-Top-Right. The operator is equipped with 8 IMUs attached to different parts of his upper body, which in turn are used to estimate his upper body pose. The velocity references for each joint of the robotic arm are generated based on the operator's pose so that the operator's resting position gives a zero velocity for all joints. Feedback from the platform to the operator is provided via a camera image projected onto the operator's smart glasses, allowing the operator to see the platform and simultaneously adopt a first-person perspective of the platform. The presented teleoperation method was successfully integrated with the MLMP platform. Before conducting the field tests, the teleoperation system was validated in simulation. Then, the platform was deployed in the power line section within the ATLAS Center. The operator was able to install there the clip-type bird diverters three times without any failure.

The deployment of MLMP represents the first demonstration of an efficient aerial robotic system combining flight and rolling with both autonomy and teleoperation capabilities, vali-

Figure 11: Top) Clip-type bird diverter end effector and installation with MLMP using IMU-based teleoperation method. Bottom-left) Charging station at the end effector. Bottom-center) Fully integrated system of the lightweight charging station (1 - electronics compartment; 2 - split-core current transformer; 3 - V-shaped landing station). Bottom-right) Charging station integrated on HolyBro QAV250 quadrotor, which is used as a proof-of-concept drone to demonstrate the charging of the drone with the developed charging station.

dated through the installation of devices on power lines (including heavy battery chargers).

7 Aerial Co-Working Methods and Results

7.1 Gesture Recognition

In aerial co-working scenarios, human worker-UAV interaction and collaboration are critical. In this direction, we developed a human worker detection and gesture recognition system that can run smoothly onboard the platforms from Section 4.3, enabling visual communication between human workers and aerial robots via gestures. First, RGB images from the onboard camera are online processed for human detection and tracking. A fast deep neural object detector based on Single-Shot Detector (SSD) [58] is employed in combination with a custom LDES-ODDA (Large Displacement tracking via Estimation of Similarity) visual tracker. The output of this pipeline is a predicted bounding box for the tracked human in each input image where the human is visible, as depicted in Figure 12-top. The predicted bounding boxes are then used in the gesture recognition pipeline. To maximize human worker detection accuracy, both the detector and the tracker were pre-trained on a manually annotated dataset[7] and then fine-tuned using videos of a human operator wearing safety equipment.

Given a sequence of images captured by an RGB camera of the UAV and the corresponding bounding boxes of the tracked human, the gesture recognition module recognizes the performed

[7] https://aiia.csd.auth.gr/open-multidrone-datasets

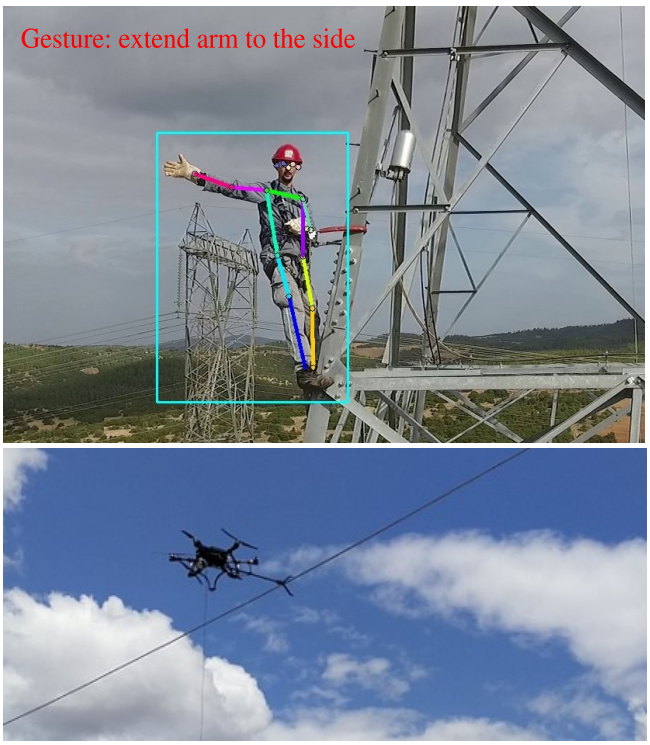

Figure 12: Top) Visualization of all outputs (bounding box, 2D skeleton, predicted gesture) of the developed gesture recognition pipeline overlaid on the corresponding input video frame. Bottom) Picture of drone-based power line voltage check performed in ATLAS. The measured potential is compared to that of a ground cable to obtain the power line voltage, which is displayed on the ground station for the operator.

gestures from a predefined set (e.g., extend one arm to the side). The gesture recognition proceeds as a sequential pipeline. First, each video frame is cropped using the corresponding bounding box of the tracked human worker. Then, our method, as described in [59], extracts a 2D human skeleton from each input image in pixel coordinates. The last outputs of the skeleton extractor is processed by a gesture classifier [32], a lightweight Long Short-Term Memory (LSTM) neural architecture that predicts the type of the performed gesture. The pipeline was trained on a large, manually annotated dataset of gestures[8], and was further fine-tuned to perform effectively on aerial images.

The developed gesture recognition pipeline was specifically designed to be simple and effective, since it must be run onboard the ACW-D, using lightweight components for this purpose: SSD for human detection, lightweight CNN for 2D human skeleton extraction, and lightweight LSTM for final gesture classification. These components are combined in a novel and effective configuration that ensures increased gesture recognition performance.

More specifically, the SSD is combined with the custom LDES-ODDA visual tracker adopting a unified detection-and-tracking configuration in which detection and tracking are performed alternately, combining the strengths of both approaches to achieve higher accuracy and fast inference. Regarding the 2D human skeleton extraction CNN, our previous method [60] has been improved by replacing the simple interbranch skip connections with more powerful cross-attention synapses [61] that enhanced its 2D skeleton extraction performance, as can be seen in Table 9. Finally, in order to ensure that the employed LSTM gesture classifier is properly fed with inputs during ACW-D operation, the last N outputs of the skeleton extractor, covering N successive video frames, are stored in a FIFO buffer that is updated with a newly extracted 2D skeleton every k video frame. This buffer is subsequently processed by the LSTM gesture classi-

[8] `https://aiia.csd.auth.gr/auth-uav-gesture-dataset`

fier that predicts the type of the performed gesture. The parameters N and k were empirically tuned to $N = 9$ and $k = 1$, based on the camera's update rate and the pipeline's performance when running onboard the ACW-D. A quantitative comparison of our gesture classifier with other lightweight approaches can be seen in Table 10.

All the contributions above ensure that the overall proposed gesture recognition configuration is robust to input variations related to vibrations and different illumination or background conditions that may occur in the ACW-D-captured RGB videos, allowing it to accurately recognize the performed gestures in multiple scenarios.

Table 9: Evaluation of our 2D skeleton extractor on the COCO dataset [62]. Best method is marked in bold.

Method	**AP**
SimpleBaseline [63]	71.5
Lite-HRNet [64]	69.7
UDP [65]	72.5
CNN-GAN [60]	73.3
Ours	**74.2**

Table 10: Evaluation of our LSTM gesture classifier on AUTH UAV Gesture [22] and UAV-Gesture [21] datasets. Best method is marked in bold.

Method	**AUTH UAV Gesture** [22]	**UAV Gesture** [21]
P-CNN [66]	—	91.9%
DD-Net [67]	74.2%	91.5%
Ours	**76.0%**	**94.6%**

7.2 Voltage Checking with the ACW-V Platform

The voltage check application measures the voltage on a power line to make sure it is safe for humans to conduct maintenance tasks. To achieve this, a contact arm was integrated into the ACW-V platform, see Figure 12-Bottom. The tip's shape was designed to facilitate contact with a conductor, and it is equipped with force and potential sensors.

An impedance controller was designed to control the ACW's behavior during a physical interaction task. This control strategy modulates the robot's dynamics by imposing the desired inertia, damping, and stiffness on aerial robot behavior while in contact. This desired impedance is achieved using an admittance filter as an outer loop controller that provides reference signals to the internal loop motion controller. In particular, the admittance filter modifies the robot's reference trajectory based on the impedance parameters and sensed forces and torques, resulting in a new trajectory to be tracked by the aerial robot's internal motion controller. The choice of using an admittance filter in a hierarchical way with the motion controller allows for enhancing the motion controller for high-performance trajectory tracking in the presence of disturbances, e.g., wind. The time required to conduct the voltage check (from take-off to landing) on the power line scenario within the ATLAS Flight Center was 1 min 30 sec, with a power line at a height of 15 m.

Figure 13: Tool delivery demonstration. Left) the gesture "palms together" causes the pulley to descend. Center) the operator retrieves the tool. Right) the gesture "arm up" commands the pulley to rise.

7.3 Tool Delivery

Delivery and handover of a tool to a worker carrying out power line maintenance tasks from an elevated working platform was also validated, see Figure 13. Gesture recognition was used to command the tool delivery multi-rotor ACW-D (see Section 4.3) applying the gesture recognition system described in Section 7.1. Five different gestures were considered: i) palms together meant the pulley to go down; ii) arm up meant it to go up; iii) arms down was recognized as "no gesture" and meant stop the pulley of the delivery multi-rotor ACW-D; iv) arms crossed to abort the mission in case of an emergency; and v) arm to the side. No failure in gesture recognition was experienced in the final experiments. ACW-D flew to approximately 2 m above and 1 m next to the lift to ensure the workers' safety and distance regulations. Then, the worker gestured to the robot, which assisted the worker with the delivery and retrieval of the tool. The time to conduct delivery operation was 2 min.

7.4 Multi-UAV for Co-Worker Safety (Safe-CW)

A group of monitoring multi-rotors were used to observe the human operator to ensure adherence to the safety rules of maintenance operations. In the proposed solution, a leading UAV uses 3D LiDAR data to detect the human worker on the mobile lift platform, see Figure 14. Based on this detection, the UAV adjusts its position to provide the required field of view of the scene while the other aerial robots maintain a formation defined in relation to the position of the monitored object and the camera optical axis of the leading UAV, thereby offering additional perspectives of the monitored scene.

Individual UAVs apply a multi-stage model predictive control (MPC) based distributed cooperative motion planning approach [68], running onboard the UAVs. This approach starts with the generation of reference trajectories using a leader-follower formation scheme and the most recent trajectory of the leader UAV shared through the Wi-Fi communication channel. In the next step, a point cloud representation of the surrounding environment is generated from an onboard-built map with additional points integrated to represent the current position of other UAVs and their planned trajectories. The generated map is then used for planning a collision-free path along the original reference trajectory and the consequent generation of the safe collision-free corridor by applying convex decomposition of free space [69]. In the final step, the trajectories of the UAVs are optimized within their corresponding safe corridors and passed to reference tracker and low-level controllers for execution [70].

These Safe-CW platforms can serve as inspection robots in the same mission, assisting

the operator in getting detailed data about the power lines from various viewpoints during ongoing maintenance operations. An arbitrary number of UAVs can be tasked to switch from safety monitoring to inspection mode. Utilizing the same motion planning approach [68], the UAVs in inspection mode are navigated to the desired viewpoints while still avoiding collisions with other UAVs and obstacles. Once the inspection task is completed, the UAVs return to their designated safety monitoring positions. The whole system, relying fully on onboard computation, was extensively validated in different scenarios, including both monitoring and inspection tasks. A snapshot from the real-world validation is shown in Figure 14. The average reaction time of the system to operator and human worker request was 1.45 s and the ratio of mission time for which a view of the human worker is provided was 100% in the final experiments.

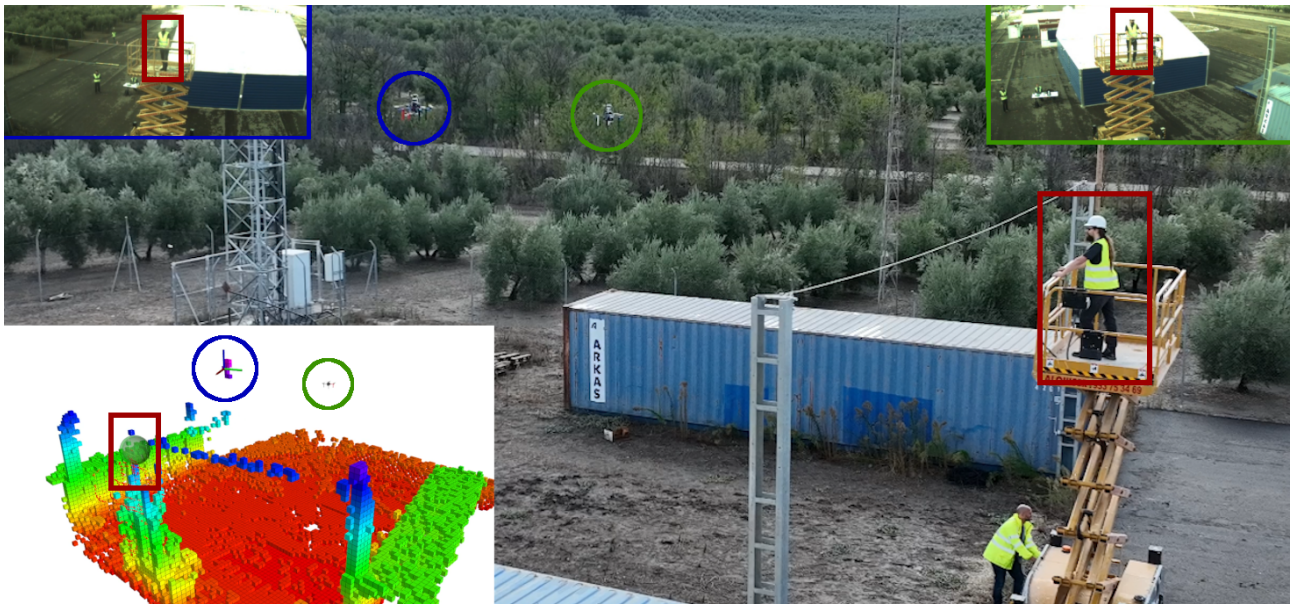

Figure 14: Snapshot showing safety monitoring of a human worker by a team of UAVs (highlighted by black and green circles). In the top corners are the images from onboard cameras of particular UAVs, while the image in the bottom left corner shows the occupancy map built from the onboard LiDAR together with the detection of the human operator (green sphere in red rectangle).

To this date, the presented aerial system represents the first aerial robotic co-working system for voltage verification, tool delivery, and multi-robot monitoring that has been demonstrated in the context of maintenance of electrical power transmission systems.

8 Lessons Learned and Recommendations for New Designs

The validation of the AERIAL-CORE system involved different platforms developed for the three application domains. From the perspective of an end user interested in using aerial robots for the I&M of power lines or any other similar linear infrastructure, the question arises as to what is the best solution or combination of platforms for a given scenario. This decision should be determined by the system designer based on the particular requirements and specifications in each case, applying principles as the ones described in the following subsections. The diversity of the platforms presented in this paper is useful in assessing how the platforms can be compared and complemented, deriving some general considerations, such as:

- The suitability of the different long-range platforms according to their purpose (3D mapping, visual or thermal inspection), the required accuracy and detail of the gathered data (fixed-wing vs hovering flight), and the ability to overcome the wind perturbations (morphing wings vs fixed-wings).

- The tradeoff between general purpose platforms like MLMP designed for installing different types of standard devices, and much lighter and smaller platforms as DARP requiring customized devices that are more suitable for the robot.

- The different ways in which aerial robots can support the activity of human workers on the power lines, with the focus on enhancing safety while operating at high altitude.

During the development of the AERIAL-CORE project, different levels of technological readiness were achieved. Only the platforms presented in Section 4 achieved a TRL above 5 (technology demonstration) and were included in the integrated system demonstrated in October 2023 at ATLAS. The methods and technologies described in Sections 5, 6, and 7 have different maturity levels, but all have demonstrated enough performance to be used in industrial inspection and maintenance.

In the following, we summarize the lessons learned in each of the three subsystems, pointing out some aspects that may be of interest for future investigation.

8.1 Long-Range Inspection

Inspection beyond the visual line of sight imposes significant safety constraints related to the reliability of the platforms and the particular scenarios. Both aspects should be considered to meet the drone regulations. We would like to point out the large time and effort required to prepare the experiments, and particularly to obtain the required permissions to fly meeting the current regulations. The long-range inspection was performed under the EASA (European Union Aviation Safety Agency) "Specific Category". The UAVs performing these flights operated under two different regulatory conditions: (1) Operational authorization in SAIL II, which grants the tilt-rotor aircraft to fly distances of up to 10 km while inspecting power lines, and (2) EASA Standard STS-ES-02 scenario, which enables multi-rotor flights to be carried out up to 2 km from the ground control station with observers and maintaining an altitude below 120 m above ground level. Although the UAV regulation is not homogeneous worldwide, the EASA operational authorization is based on SORA (Specific Operations Risk Assessment) methodology which was developed by JARUS (Joint Authorities for Rulemaking on Unmanned Systems) and has a worldwide representation. Then, AERIAL-CORE has proved that it is possible to perform long-range power line inspections with limited risk (SAIL II) in rural areas, then reducing the requirements imposed on the aerial platforms and facilitating the use of novel technologies. The use of SORA in the EASA operational authorization facilitates that the technologies used in this project could be translated to many other countries worldwide.

The application of VTOL platforms for long-range inspection is a convenient solution since these simplify the take-off compared to fixed-wing UAVs, while providing longer flight distances than multi-rotors. The long-range inspection subsystem in AERIAL-CORE was designed taking into account the need to cover large areas while providing detailed data, also considering the effect of wind, which motivated the integration of three different platforms in the validation scenario for comparative purposes. DeltaQuad is a commercial VTOL platform without morphing capability that has difficulties in overcoming significant wind perturbations, and thus it is not suitable for detailed inspections in adverse conditions. Marvin is an industrial platform that evolved during the project, incorporating the wing-morphing capability to enhance the

response to wind. Morpho is a novel platform designed following a bioinspired approach that can be applied in vertical flights to capture detailed images of devices installed in the cables and towers, which is not possible with DeltaQuad and Marvin. However, its payload, flight time and range are lower, so it should operate in a close proximity area.

The morphing platforms presented in Section 4.1 still have limitations in hovering due to the wind perturbations together with the limitations in payload which constraints the integration of high-quality sensors required for very accurate inspections and mapping, similar to those carried on manned helicopters. Hence, the combination of VTOL with multi-rotor platforms, presented in previous sections, seems to be the most appropriate solution to address this problem.

The following functionalities, presented in Section 5, were proven to be very valuable during the experimental tests:

- Power line tracking with event cameras improves the reliability against motion blur and changes in lighting conditions. Further improvements in reliability could be obtained by combining the visual tracker with the GNSS tracking by using maps with accurate information about the power lines. However, existing maps, even those provided by power line operators, contain incomplete and even wrong information. Improving these maps is definitely necessary and evidences the need for adopting technologies such as Mapper. Particularly, a better knowledge of the height of the conductors and towers is important to avoid possible collisions.

- The mapping functionality is also very valuable for the utility companies. The capability to perform on-line real-time mapping is very useful to avoid the delays of current inspection and preventive maintenance procedures. Besides, it also opens the possibility of applying aerial robots for pruning tasks. Long-range power-line mapping can face robustness challenges linked to the huge variety of types of environments that the aerial robot can traverse, which include geometrically rich environments and also areas with very low geometrical information, such as flat crop terrains with no vegetation, which can drastically degrade the accuracy of the resulting map. This has been addressed in AERIAL-CORE through the introduction of GNSS in the mapping method, originally developed using only LiDAR. One interesting research line to mitigate these issues is to consider the uncertainty of the LiDAR measurements and reflect it in the map, by considering maps with uncertainty. These methods are under-researched. Although some methods have started to consider the map uncertainty, they do not consider it in robot state estimation. The development of map representations more suitable for representing planes and that fully consider map uncertainty in all components of the mapping scheme is a very interesting research topic to robustify mapping in environments with low geometrical information content, and is object of current research.

- The inspection with a team of aerial robots decreases the total inspection time and allows the specialization of the platform decreasing the total cost when compared to very expensive high-capability platforms. The application of the multi-UAV system can be optimized by taking into account the constraints imposed by the individual platforms. Real-time wind measurements could be also applied for planning and re-planning inspection trajectories.

- Battery recharging systems can be used to extend the duration and range of the inspections. In the future, energy harvesting from the line, as presented in Section 6, can be integrated.

It has been shown that aerial robotic technologies can be integrated to perform fully autonomously the inspection of hundred kilometres of electrical transmission lines leveraging the

combination of morphing and other novel platform technologies, with software for visual tracking, semantic mapping, landing on charging platforms or the power line, and optimal multi-UAV planning taking into account the constraints of the platforms and the wind perturbations. The exploitation of this system requires demonstrating its reliability in different environmental conditions and performing risk analysis to meet the regulations in different countries.

8.2 Local Aerial Manipulation

The deployment of the robotic manipulator on the power line presented several benefits compared to the realization of the operation while flying. First of all, the positioning accuracy of the end effector is significantly improved, resulting in higher success rates and shorter execution times. It also improves the energy consumption when rolling along the line for installing several devices. The three main inconveniences are: 1) the increase in the overall weight of the platform due to the perching mechanism and the rolling base, 2) the need to perform the perching and take-off maneuvers from the line, and 3) the reduction in the effective workspace for the manipulator due to the relative configuration of the manipulator with respect to the power line imposed by the perching mechanism. Overall, in practice, the adopted solution is safer and more reliable than conducting the installation of devices while flying.

The experiments presented in Section 6 validated the design of the DARP and its application to the installation of lightweight devices (less than 0.5 kg), such as custom-made bird flight diverters, while rolling along the power line. On the other hand, the general-purpose MLMP can be applied to the installation of different types of devices, including standard bird diverters, electrical spaces, and recharging stations, as required in the specifications of the project. This is achieved at expenses of increasing the weight and installation time by one order of magnitude with respect to the DARP. The size and weight of the platforms have implications for their transport by motor vehicles (vans) and for obtaining the flight permits.

The combination of LiDAR and RTK-GPS is a suitable solution for positioning accurately the aerial robot in the power line scenario, taking into account the good visibility conditions for GNSS sensors in this application and the significant reduction in the weight and cost of LiDAR technology.

The ground vehicle equipped with an elevated working platform employed by the human operators that provided support during the realization of the flight tests on the power line (Figure 1) got stuck in the mud due to the rain from the previous night. This evidenced some of the inconveniences of this kind of heavy vehicle extensively employed in power line maintenance, along with the risk involved for the workers when standing several meters above the ground.

The following recommendations are provided for the development and application of aerial manipulators for power line maintenance operations:

- The deployment of the robot manipulators on power lines to conduct maintenance operations can be done from above or from below, although the latter is more convenient as there is no constraint on the upper altitude, the detachment of the multi-rotor from below is a bit more tricky operation.

- The actuator of the rolling base should be powerful and robust enough to move the robot along the power line overcoming its weight and the sag of the line. The drive wheel should provide enough friction to avoid the slippage on the cable.

- Reducing the overall weight of the deployed manipulation platform is convenient to reduce the deflection (sag) of the power line caused by the weight of the robot, which tends to increase the pitch angle for rolling base.

- V-shaped frames are particularly useful to facilitate the alignment of the rolling base with the cable during the deployment manoeuvre. The preloaded hook-handle mechanism is also a simple but effective solution to detach the robot manipulator from the aerial platform.

- For the cable-suspended hook mechanism used to retrieve the deployed manipulator, it is convenient that the cables present certain stiffness and weight to avoid their oscillation due to the wind or the aerodynamic downwash effect. The hook should be designed in a way that facilitates the passive grasping of the handle in a reliable way.

8.3 Aerial Robotic Co-Workers

Aerial robotics technologies intended to help human workers at height have been developed and tested in the field. These include visual detection and tracking of the workers, autonomous guidance of the aerial robots via recognized gestures, the performance of dangerous activities, such as voltage checks, the physical interaction for tool delivery, and the coordinated motion of several UAVs for co-worker safety. Fully actuated platforms have demonstrated to provide suitable properties for interaction, but still, more safety tests should be conducted before real application with human workers. The early definition of the project specifications relative to the aerial co-working activities was essential to investigate the involved human-robot physical interactions while flying and to design appropriate platforms for this purpose. The fully-actuated multi-rotor configuration is particularly suitable for this purpose due to its ability to generate 6-DOF wrenches that compensate the forces and moments exerted by the human worker in aerial handover tasks. It is also desirable that the size and weight of these platforms are as low as possible for safety reasons and to simplify their transportation. The delivery of tools or devices through a cable-suspended mechanism (see Figure 13) also reduces the risk of collision of the aerial robot with the human operator.

Novel aerial co-worker robots designed to collaborate with human workers in the realization of maintenance operations should account for the following aspects:

- Use of platforms with less noise, light signals, and intrinsic safety, such as the protection of the propellers.

- Training and validation in many conditions and scenarios to increase the reliability of perception functionalities.

- Training of human workers and working with the utility companies to obtain the relevant permits.

- Use of multiple perception modalities to achieve redundancy, increases the reliability of human worker detection and gesture recognition algorithms, and prevents false positive detection of gestures resulting in potentially dangerous situations.

- Use of multi-layer safety mechanisms including redundant source of data to prevent collision with a human worker.

- Design of the navigation algorithms such that the behavior of co-worker UAVs provides clear feedback to the human worker about successful detection and recognition of a gesture, preventing repeated unintentional requests.

9 Conclusion

The relevance and interest of intelligent aerial robotic systems and their application to I&M of electrical power distribution systems have been demonstrated for the first time in this paper. The presented system includes UAVs capable of performing VTOL, completing detailed inspections at low velocity or hovering and morphing to minimize energy consumption during long-range inspection.

The morphing drone technology demonstrated better capabilities than conventional UAVs improving stability, maneuverability, and energy efficiency in challenging conditions. While results indicate advantages over conventional UAVs, further development is needed for commercial applications. Key areas for improvement include optimizing actuation speed for real-time responsiveness, refining control strategies for stability in highly dynamic environments, and enhancing structural robustness for prolonged operations. These, among other refinements, will be crucial for transforming morphing technology into robust, commercial products which will enhance UAV performance in demanding applications, significantly impacting the power and energy sectors by enabling safer, more efficient inspections and maintenance operations.

Multiple heterogeneous intelligent aerial robots flying BVLOS under international and national civil regulations have shown the ability to inspect hundreds of kilometers of power lines cooperatively. Further, aerial robots are able to perform autonomous tracking of the lines and mapping of the vegetation near the lines, which is very important to avoid forest fires. They can also perch on the lines to recharge the battery or to realize maintenance tasks using robotic manipulators, including the installation of bird diverters to protect natural life. The aerial manipulators that we have presented are the first of their kind able to land on cables of real electrical power lines and perform manipulation involving significant forces. The paper has also presented the first aerial robotic co-workers helping human operators inspect and maintain electrical lines. The designed aerial robots are capable of helping human workers at high altitudes by measuring the voltage of the line, providing them with tools and monitoring their safety.

A video with a summary of the AERIAL-CORE project can be found at `https://www.youtube.com/watch?v=Oyw7VwM7sCs`. The metrics presented in this paper can be used by researchers and engineers to compare the performance of new systems. The expected impact of this work is very high because the I&M of electrical power lines has a cost of many billions in the world (more than 2.2 billion Euro only in Europe), and there is also a direct impact on the safety of the workers. The above applications have many potential follow-ups including, for example, the application of Generative AI to facilitate human interaction, and the complete integration of the three subsystems in the field.

The work presented in this paper can also open new paths, such as implementing drone highways over the power lines, with the robots perching on the line to charge batteries. The technologies derived from the AERIAL-CORE project can be transferred to other application domains involving the inspection and maintenance of large linear infrastructures that can benefit from the use of aerial robots. For example, the long-range inspection platforms described in Section 4.1 and the methods presented in Section 5 can be applied to the inspection of railways, highways, or pipelines in large chemical plants to detect cracks and other defects. The aerial transportation, deployment, and retrieval of lightweight manipulators capable of perching and rolling along the workspace opens new possibilities for long-term operations in power lines, wind turbines, pipelines, and construction sites, for example, for painting or cleaning the facades of the buildings using cable-suspended aerial manipulators. Aerial co-working robots, as the ones presented in Section 7, may become useful in other high altitude I&M scenarios shared with humans, like wind farms and also in construction sites.

Acknowledgment

This work was supported by the EU Horizon 2020 Research and Innovation Program under grant agreement no. 871479 (AERIAL-CORE: AERIAL COgnitive integrated multi-task Robotic system with Extended operation range and safety).

References

[1] J. Cacace, S. M. Orozco-Soto, A. Suarez, A. Caballero, M. Orsag, S. Bogdan, G. Vasiljevic, E. Ebeid, J. A. A. Rodriguez, and A. Ollero, "Safe local aerial manipulation for the installation of devices on power lines: Aerial-core first year results and designs," *Applied Sciences*, vol. 11, no. 13, p. 6220, 2021.

[2] A. Ollero, M. Tognon, A. Suarez, D. Lee, and A. Franchi, "Past, present, and future of aerial robotic manipulators," *IEEE Transactions on Robotics*, vol. 38, no. 1, pp. 626–645, 2021.

[3] A. B. Alhassan, X. Zhang, H. Shen, and H. Xu, "Power transmission line inspection robots: A review, trends and challenges for future research," *International Journal of Electrical Power & Energy Systems*, vol. 118, p. 105862, 2020.

[4] L. Yang, J. Fan, Y. Liu, E. Li, J. Peng, and Z. Liang, "A review on state-of-the-art power line inspection techniques," *IEEE Transactions on Instrumentation and Measurement*, vol. 69, no. 12, pp. 9350–9365, 2020.

[5] J. Katrasnik, F. Pernus, and B. Likar, "A survey of mobile robots for distribution power line inspection," *IEEE Transactions on power delivery*, vol. 25, no. 1, pp. 485–493, 2009.

[6] M. Chen, Y. Tian, S. Xing, Z. Li, E. Li, Z. Liang, and R. Guo, "Environment perception technologies for power transmission line inspection robots," *Journal of Sensors*, vol. 2021, no. 1, p. 5559231, 2021.

[7] A. Ollero, G. Heredia, A. Franchi, G. Antonelli, K. Kondak, A. Sanfeliu, A. Viguria, J. R. Martinez-de Dios, F. Pierri, J. Cortés *et al.*, "The aeroarms project: Aerial robots with advanced manipulation capabilities for inspection and maintenance," *IEEE Robotics & Automation Magazine*, vol. 25, no. 4, pp. 12–23, 2018.

[8] A. Suarez, J. Cacace, and M. Orsag, "Aerial robotics for inspection and maintenance: special issue editorial," p. 3583, 2022.

[9] M. Car, L. Markovic, A. Ivanovic, M. Orsag, and S. Bogdan, "Autonomous wind-turbine blade inspection using lidar-equipped unmanned aerial vehicle," *IEEE access*, vol. 8, pp. 131 380–131 387, 2020.

[10] A. Caballero, F. J. Roman-Escorza, I. Maza, and A. Ollero, "A multi-uav route planning method for fast inspection of electric power transmission lines," in *2024 International Conference on Unmanned Aircraft Systems (ICUAS)*. IEEE, 2024, pp. 835–842.

[11] J. L. Paneque, J. R. Martínez-de Dios, A. Ollero, D. Hanover, S. Sun, A. Romero, and D. Scaramuzza, "Perception-aware perching on powerlines with multirotors," *IEEE Robotics and Automation Letters*, vol. 7, no. 2, pp. 3077–3084, 2022.

[12] J. Xing, G. Cioffi, J. Hidalgo-Carrió, and D. Scaramuzza, "Autonomous power line inspection with drones via perception-aware MPC," *2023 IEEE/RSJ International Conference on Intelligent Robots and Systems (IROS)*, 2023.

[13] V. Valseca, J. Paneque, J. Martínez-de Dios, and A. Ollero, "Real-time lidar-based semantic classification for powerline inspection," in *2022 International Conference on Unmanned Aircraft Systems (ICUAS)*. IEEE, 2022, pp. 478–486.

[14] J. Luna-Santamaria, I. G. Rodríguez, J. M.-d. Dios, and A. Ollero, "Accurate lidar-based semantic classification for powerline inspection," in *International Work-Conference on the Interplay Between Natural and Artificial Computation*. Springer, 2024, pp. 215–224.

[15] A. Suarez, R. Salmoral, P. J. Zarco-Periñan, and A. Ollero, "Experimental evaluation of aerial manipulation robot in contact with 15 kv power line: Shielded and long reach configurations," *IEEE Access*, vol. 9, pp. 94 573–94 585, 2021.

[16] M. Skriver, A. Stengaard, U. P. Schultz, and E. Ebeid, "Experimental investigation of emc weaknesses in uavs during overhead power line inspection," in *2022 International Conference on Unmanned Aircraft Systems (ICUAS)*. IEEE, 2022, pp. 626–635.

[17] W. Stewart, D. Floreano, and E. Ebeid, "A lightweight device for energy harvesting from power lines with a fixed-wing uav," in *2022 International Conference on Unmanned Aircraft Systems (ICUAS)*. IEEE, 2022, pp. 86–93.

[18] F. F. Nyboe, N. H. Malle, V. D. Hoang, and E. Ebeid, "Open-source hardware/software architecture for autonomous powerline-aware drone navigation and recharging," in *2023 International Conference on Unmanned Aircraft Systems (ICUAS)*. IEEE, 2023, pp. 1233–1240.

[19] A. Afifi, M. van Holland, and A. Franchi, "Toward physical human-robot interaction control with aerial manipulators: Compliance, redundancy resolution, and input limits," in *2022 International Conference on Robotics and Automation (ICRA)*. IEEE, 2022, pp. 4855–4861.

[20] A. Suarez, R. Salmoral, A. Garofano-Soldado, G. Heredia, and A. Ollero, "Aerial device delivery for power line inspection and maintenance," in *2022 International Conference on Unmanned Aircraft Systems (ICUAS)*. IEEE, 2022, pp. 30–38.

[21] A. G. Perera, Y. Wei Law, and J. Chahl, "Uav-gesture: A dataset for uav control and gesture recognition," in *Proceedings of the European Conference on Computer Vision (ECCV) Workshops*, 2018, pp. 0–0.

[22] F. Patrona, I. Mademlis, and I. Pitas, "An overview of hand gesture languages for autonomous uav handling," *2021 Aerial Robotic Systems Physically Interacting with the Environment (AIRPHARO)*, pp. 1–7, 2021.

[23] A. Suarez, S. R. Nekoo, and A. Ollero, "Ultra-lightweight anthropomorphic dual-arm rolling robot for dexterous manipulation tasks on linear infrastructures: A self-stabilizing system," *Mechatronics*, vol. 94, p. 103021, 2023.

[24] A. Suarez, V. M. Vega, M. Fernandez, G. Heredia, and A. Ollero, "Benchmarks for aerial manipulation," *IEEE Robotics and Automation Letters*, vol. 5, no. 2, pp. 2650–2657, 2020.

[25] D. Gayango, R. Salmoral, H. Romero, J. M. Carmona, A. Suarez, and A. Ollero, "Benchmark evaluation of hybrid fixed-flapping wing aerial robot with autopilot architecture for autonomous outdoor flight operations," *IEEE Robotics and Automation Letters*, vol. 8, no. 7, pp. 4243–4250, 2023.

[26] A. Suarez and A. Ollero, "Dual arm aerial manipulation while flying, holding and perching: Comparative case study," in *Iberian Robotics conference*. Springer, 2022, pp. 259–270.

[27] C. Vourtsis, V. C. Rochel, N. S. Müller, W. Stewart, and D. Floreano, "Wind Defiant Morphing Drones," *Advanced Intelligent Systems*, vol. 5, no. 3, p. 2200297.

[28] C. Vourtsis, "Resilient drones with morphing wings," Ph.D. dissertation, EPFL, Lausanne, 2023.

[29] C. Vourtsis, V. C. Rochel, N. S. Müller, W. Stewart, and D. Floreano, "Wind defiant morphing drones," *Advanced Intelligent Systems*, vol. 5, no. 3, p. 2200297, 2023.

[30] M. Gil-Castilla, A. Caballero, I. Maza, and A. Ollero, "Integration of customized commercial uav s with open-source tools in a heterogeneous multi-uav system for power-lines inspection," in *2024 International Conference on Unmanned Aircraft Systems (ICUAS)*. IEEE, 2024, pp. 1362–1369.

[31] J. Marredo, A. Petrus, M. Trujillo, A. Viguria, and A. Ollero, "A novel unmanned aerial system for power line inspection and maintenance operations," in *2024 International Conference on Unmanned Aircraft Systems (ICUAS)*. IEEE, 2024, pp. 602–609.

[32] C. Papaioannidis, D. Makrygiannis, I. Mademlis, and I. Pitas, "Learning Fast and Robust Gesture Recognition," in *Proc. of the EURASIP European Conference on Signal Processing*, 2021, pp. 761–765.

[33] A. Dietsche, G. Cioffi, J. Hidalgo-Carrió, and D. Scaramuzza, "Powerline tracking with event cameras," in *2021 IEEE/RSJ International Conference on Intelligent Robots and Systems (IROS)*. IEEE, 2021, pp. 6990–6997.

[34] J. Redmon, S. Divvala, R. Girshick, and A. Farhadi, "You only look once: Unified, real-time object detection," in *Proc. of the IEEE conference on computer vision and pattern recognition*, 2016, pp. 779–788.

[35] B. D. Lucas and T. Kanade, "An iterative image registration technique with an application to stereo vision," in *IJCAI'81: 7th international joint conference on Artificial intelligence*, vol. 2, 1981, pp. 674–679.

[36] K. Zhao, Q. Han, C.-B. Zhang, J. Xu, and M.-M. Cheng, "Deep hough transform for semantic line detection," *IEEE Transactions on Pattern Analysis and Machine Intelligence*, vol. 44, no. 9, pp. 4793–4806, 2021.

[37] X. Pan, J. Shi, P. Luo, X. Wang, and X. Tang, "Spatial as deep: Spatial cnn for traffic scene understanding," in *Proceedings of the AAAI conference on artificial intelligence*, vol. 32, no. 1, 2018.

[38] L. Tabelini, R. Berriel, T. M. Paixao, C. Badue, A. F. De Souza, and T. Oliveira-Santos, "Keep your eyes on the lane: Real-time attention-guided lane detection," in *Proceedings of the IEEE/CVF conference on computer vision and pattern recognition*, 2021, pp. 294–302.

[39] L. Liu, X. Chen, S. Zhu, and P. Tan, "Condlanenet: a top-to-down lane detection framework based on conditional convolution," in *Proceedings of the IEEE/CVF international conference on computer vision*, 2021, pp. 3773–3782.

[40] X. Li, J. Li, X. Hu, and J. Yang, "Line-cnn: End-to-end traffic line detection with line proposal unit," *IEEE Transactions on Intelligent Transportation Systems*, vol. 21, no. 1, pp. 248–258, 2019.

[41] Z. Chen, Q. Liu, and C. Lian, "Pointlanenet: Efficient end-to-end cnns for accurate real-time lane detection," in *2019 IEEE intelligent vehicles symposium (IV)*. IEEE, 2019, pp. 2563–2568.

[42] L. Everding and J. Conradt, "Low-latency line tracking using event-based dynamic vision sensors," *Frontiers in neurorobotics*, vol. 12, p. 4, 2018.

[43] G. Gallego, T. Delbruck, G. Orchard, C. Bartolozzi, B. Taba, A. Censi, S. Leutenegger, A. Davison, J. Conradt, K. Daniilidis, and D. Scaramuzza, "Event-based vision: A survey," 2020.

[44] P. Foehn, E. Kaufmann, A. Romero, R. Penicka, S. Sun, L. Bauersfeld, T. Laengle, G. Cioffi, Y. Song, A. Loquercio *et al.*, "Agilicious: Open-source and open-hardware agile quadrotor for vision-based flight," *Science robotics*, vol. 7, no. 67, p. eabl6259, 2022.

[45] D. Falanga, P. Foehn, P. Lu, and D. Scaramuzza, "Pampc: Perception-aware model predictive control for quadrotors," in *2018 IEEE/RSJ International Conference on Intelligent Robots and Systems (IROS)*. IEEE, 2018, pp. 1–8.

[46] W. Xu, Y. Cai, D. He, J. Lin, and F. Zhang, "Fast-lio2: Fast direct lidar-inertial odometry," *IEEE Transactions on Robotics*, pp. 1–21, 2022.

[47] J. Paneque, V. Valseca, J. Martínez-de Dios, and A. Ollero, "Autonomous reactive lidar-based mapping for powerline inspection," in *2022 International Conference on Unmanned Aircraft Systems (ICUAS)*. IEEE, 2022, pp. 962–971.

[48] C. R. Qi, L. Yi, H. Su, and L. J. Guibas, "Pointnet++: Deep hierarchical feature learning on point sets in a metric space," *Advances in neural information processing systems*, vol. 30, 2017.

[49] G. Laporte, "The traveling salesman problem: An overview of exact and approximate algorithms," *European Journal of Operational Research*, vol. 59, no. 2, pp. 231–247, 1992.

[50] A. Suarez, G. Heredia, and A. Ollero, "Design of an anthropomorphic, compliant, and lightweight dual arm for aerial manipulation," *IEEE Access*, vol. 6, pp. 29 173–29 189, 2018.

[51] M. Bisgaard, J. D. Bendtsen, and A. la Cour-Harbo, "Modeling of generic slung load system," *Journal of guidance, control, and dynamics*, vol. 32, no. 2, pp. 573–585, 2009.

[52] A. Yiğit, L. Cuvillon, M. A. Perozo, S. Durand, and J. Gangloff, "Dynamic control of a macro–mini aerial manipulator with elastic suspension," *IEEE Transactions on Robotics*, vol. 39, no. 6, pp. 4820–4836, 2023.

[53] G. D'Ago, M. Selvaggio, A. Suarez, F. J. Gañán, L. R. Buonocore, M. Di Castro, V. Lippiello, A. Ollero, and F. Ruggiero, "Modelling and identification methods for simulation of cable-suspended dual-arm robotic systems," *Robotics and Autonomous Systems*, vol. 175, p. 104643, 2024.

[54] A. Suarez, A. Gonzalez-Morgado, and A. Ollero, "Lightweight and compliant bilateral teleoperation system with anthropomorphic arms for aerial and ground service operations," in *2024 IEEE International Conference on Robotics and Automation (ICRA)*. IEEE, 2024, pp. 15 685–15 691.

[55] M. Marolla, J. Cacace, and V. Lippiello, "Design and control of a novel high payload light arm for heavy aerial manipulation tasks," in *Proc. of the 20th International Conference on Informatics in Control, Automation and Robotics*, vol. 1, 2023.

[56] D. Stuhne, V. D. Hoang, G. Vasiljevic, S. Bogdan, Z. Kovacic, A. Ollero, and E. S. M. Ebeid, "Design of a wireless drone recharging station and a special robot end effector for installation on a power line," *IEEE Access*, vol. 10, pp. 88 719–88 737, 2022.

[57] V. D. Hoang and E. Ebeid, "Advanced magnetic energy harvester for charging drones from overhead powerlines," in *2023 25th European Conference on Power Electronics and Applications (EPE'23 ECCE Europe)*. IEEE, 2023, pp. 1–9.

[58] W. Liu, D. Anguelov, D. Erhan, C. Szegedy, S. Reed, C.-Y. Fu, and A. C. Berg, "SSD: Single Shot MultiBox Detector," in *Proc. of the European Conference on Computer Vision*, 2016, pp. 21–37.

[59] C. Papaioannidis, I. Mademlis, and I. Pitas, "Fast CNN-based Single-Person 2D Human Pose Estimation for Autonomous Systems," *In IEEE Transactions on Circuits and Systems for Video Technology*, vol. 33, no. 3, pp. 1262–1275, 2023.

[60] C. Papaioannidi, I. Mademlis, and I. Pitas, "Fast cnn-based single-person 2d human pose estimation for autonomous systems," *IEEE Transactions on Circuits and Systems for Video Technology*, vol. 33, no. 3, pp. 1262–1275, 2023.

[61] A. Vaswani, N. Shazeer, N. Parmar, J. Uszkoreit, L. Jones, A. N. Gomez, Ł. Kaiser, and I. Polosukhin, "Attention is all you need," *Advances in neural information processing systems*, vol. 30, 2017.

[62] T.-Y. Lin, M. Maire, S. Belongie, J. Hays, P. Perona, D. Ramanan, P. Dollár, and C. L. Zitnick, "Microsoft coco: Common objects in context," in *Computer vision–ECCV 2014: 13th European conference, zurich, Switzerland, September 6-12, 2014, proceedings, part v 13*. Springer, 2014, pp. 740–755.

[63] B. Xiao, H. Wu, and Y. Wei, "Simple baselines for human pose estimation and tracking," in *Proceedings of the European conference on computer vision (ECCV)*, 2018, pp. 466–481.

[64] C. Yu, B. Xiao, C. Gao, L. Yuan, L. Zhang, N. Sang, and J. Wang, "Lite-hrnet: A lightweight high-resolution network," in *Proceedings of the IEEE/CVF conference on computer vision and pattern recognition*, 2021, pp. 10 440–10 450.

[65] J. Huang, Z. Zhu, F. Guo, and G. Huang, "The devil is in the details: Delving into unbiased data processing for human pose estimation," in *Proceedings of the IEEE/CVF conference on computer vision and pattern recognition*, 2020, pp. 5700–5709.

[66] G. Chéron, I. Laptev, and C. Schmid, "P-cnn: Pose-based cnn features for action recognition," in *Proceedings of the IEEE international conference on computer vision*, 2015, pp. 3218–3226.

[67] F. Yang, Y. Wu, S. Sakti, and S. Nakamura, "Make skeleton-based action recognition model smaller, faster and better," in *Proceedings of the 1st ACM International Conference on Multimedia in Asia*, 2019, pp. 1–6.

[68] V. Kratky, A. Alcantara, J. Capitan, P. Štěpán, M. Saska, and A. Ollero, "Autonomous aerial filming with distributed lighting by a team of unmanned aerial vehicles," *IEEE Robotics and Automation Letters*, vol. 6, no. 4, pp. 7580–7587, 2021.

[69] S. Liu, M. Watterson, K. Mohta, K. Sun, S. Bhattacharya, C. J. Taylor, and V. Kumar, "Planning dynamically feasible trajectories for quadrotors using safe flight corridors in 3-D complex environments," *IEEE RA-L*, vol. 2, no. 3, pp. 1688–1695, 2017.

[70] T. Baca, M. Petrlik, M. Vrba, V. Spurny, R. Penicka, D. Hert, and M. Saska, "The MRS UAV System: Pushing the Frontiers of Reproducible Research, Real-world Deployment, and Education with Autonomous Unmanned Aerial Vehicles," *Journal of Intelligent & Robotic Systems*, vol. 102, no. 26, pp. 1–28, May 2021. [Online]. Available: https://link.springer.com/article/10.1007/s10846-021-01383-5